Biogeosciences

Air–sea CO$_2$ fluxes in the East China Sea based on multiple-year underway observations

X.-H. Guo[1], W.-D. Zhai[1,2], M.-H. Dai[1], C. Zhang[1], Y. Bai[3], Y. Xu[1], Q. Li[1], and G.-Z. Wang[1]

[1]State Key Laboratory of Marine Environmental Science, Xiamen University, 361102 Xiamen, China
[2]National Environmental Monitoring Center, 116023 Dalian, China
[3]State Key Laboratory of Satellite Ocean Environment Dynamics, Second Institute of Oceanography, State Oceanic Administration, 310012 Hangzhou, China

Correspondence to: M.-H. Dai (mdai@xmu.edu.cn)

Abstract. This study reports the most comprehensive data set thus far of surface seawater pCO$_2$ (partial pressure of CO$_2$) and the associated air–sea CO$_2$ fluxes in a major ocean margin, the East China Sea (ECS), based on 24 surveys conducted in 2006 to 2011. We showed highly dynamic spatial variability in sea surface pCO$_2$ in the ECS except in winter, when it ranged across a narrow band of 330 to 360 µatm. We categorized the ECS into five different domains featuring with different physics and biogeochemistry to better characterize the seasonality of the pCO$_2$ dynamics and to better constrain the CO$_2$ flux. The five domains are (I) the outer Changjiang estuary and Changjiang plume, (II) the Zhejiang–Fujian coast, (III) the northern ECS shelf, (IV) the middle ECS shelf, and (V) the southern ECS shelf. In spring and summer, pCO$_2$ off the Changjiang estuary was as low as < 100 µatm, while it was up to > 400 µatm in autumn. pCO$_2$ along the Zhejiang–Fujian coast was low in spring, summer and winter (300 to 350 µatm) but was relatively high in autumn (> 350 µatm). On the northern ECS shelf, pCO$_2$ in summer and autumn was > 340 µatm in most areas, higher than in winter and spring. On the middle and southern ECS shelf, pCO$_2$ in summer ranged from 380 to 400 µatm, which was higher than in other seasons (< 350 µatm). The area-weighted CO$_2$ flux on the entire ECS shelf was -10.0 ± 2.0 in winter, -11.7 ± 3.6 in spring, -3.5 ± 4.6 in summer and -2.3 ± 3.1 mmol m^{-2} d^{-1} in autumn. It is important to note that the standard deviations in these flux ranges mostly reflect the spatial variation in pCO$_2$ rather than the bulk uncertainty. Nevertheless, on an annual basis, the average CO$_2$ influx into the entire ECS shelf was 6.9 ± 4.0 mmol m^{-2} d^{-1}, about twice the global average in ocean margins.

1 Introduction

With the rapid growth of carbon flux measurements during the past decade, our estimation of the coastal ocean air–sea CO$_2$ fluxes is that they have converged to about 0.2 to 0.5 Pg C yr^{-1} on a global scale (Borges et al., 2005; Cai et al., 2006; Chen and Borges, 2009; Chen et al., 2013; Dai et al., 2013; Laruelle et al., 2010; Laruelle et al., 2014), and it is safe to state that the earlier estimate of up to 0.9 to 1.0 Pg C yr^{-1} was an overestimate. Having stated this, it remains, however, challenging to reliably assess the carbon fluxes in individual coastal systems that are often characterized by the greatest spatial and temporal variations (Cai and Dai, 2004; Dai et al., 2013; Dai et al., 2009; Zhai et al., 2013). Understanding regional fluxes and controls is important because it not only affects global flux estimation but also improves our capability of modelling the coastal ocean carbon cycle. A regional climate model that is particularly relevant to the societal sustainability would need an improved estimate of regional carbon fluxes to resolve its predictability of future changes. Finally, many coastal oceans have been impacted by anthropogenic activities, the signals of which remain, however, challenging to decipher (Chou et al., 2007; Omar et al., 2003).

The East China Sea (ECS) is a shelf system characterized by significant terrestrial input from one of the world's major

rivers from the west, the Changjiang (Yangtze River), as well as dynamic exchange on its eastern board with the Kuroshio, a major western ocean boundary current (Chen and Wang, 1999). Located in the temperate zone, the ECS is also characterized by a clear seasonal pattern with a warm and productive summer and a cold and less productive winter (Gong et al., 2003; Han et al., 2013). Such a dynamic nature regarding both physical circulation and biogeochemistry makes for large contrasts in different zones within the ECS, and, thus, zonally based assessment is critical to reliably constrain the CO_2 flux in time and space in this important marginal sea.

Prior studies have already revealed that the ECS is overall an annual net sink of atmospheric CO_2, with significant seasonal variations (Chou et al., 2009; Chou et al., 2011; Kim et al., 2013; Peng et al., 1999; Shim et al., 2007; Tseng et al., 2011; Tsunogai et al., 1999; Wang et al., 2000; Zhai and Dai, 2009). The ranges of present estimates are -3.3 to -6.5 in spring, -2.4 to -4.8 in summer, 0.4 to 2.9 in autumn and -13.7 to -10.4 mmol m^{-2} d^{-1} in winter. However, these estimates are either based on limited (only one or a few) field surveys (Chou et al., 2009; Chou et al., 2011; Peng et al., 1999; Shim et al., 2007; Tsunogai et al., 1999; Wang et al., 2000) or suffer from spatial limitations (Kim et al., 2013; Shim et al., 2007; Tsunogai et al., 1999; Zhai and Dai, 2009). Tseng et al. (2011) investigate the Changjiang diluted water induced CO_2 uptake in summer and obtain an empirical algorithm of surface water pCO_2 (partial pressure of CO_2) with the Changjiang discharge and sea surface temperature (SST). Subsequently, they extrapolate the empirical algorithm to the entire ECS shelf and the whole year to obtain a significant CO_2 sink of 6.3 ± 1.1 mmol m^{-2} d^{-1} (Tseng et al., 2011). With data from three field surveys conducted in spring, autumn and winter added, Tseng et al. (2014) update the annual CO_2 flux in the ECS to be -4.9 ± 1.4 mmol m^{-2} d^{-1}, using a similar empirical algorithm method.

In this study, we investigated the air–sea CO_2 fluxes on the entire ECS shelf based on large-scale observations of 24 mapping cruises from 2006 to 2011, resolving both spatial coverage and fully seasonal variations. This data set, the largest thus far, allowed for a better constraint of the carbon fluxes in this important ocean margin system. The estimate in an individual survey was based on the gridded average values in five physically and biogeochemically distinct domains (Fig. 1), based on which the distribution of the pCO_2 and the major controls in the ECS were better revealed and the air–sea CO_2 fluxes were better estimated.

2 Study area

The ECS is one of the major marginal seas located in the western Pacific. The largest freshwater source for the ECS is the Changjiang, which delivers 940 km^3 freshwater annually, with the highest discharge in summer (Dai and Trenberth, 2002). The circulation of the ECS is modulated by
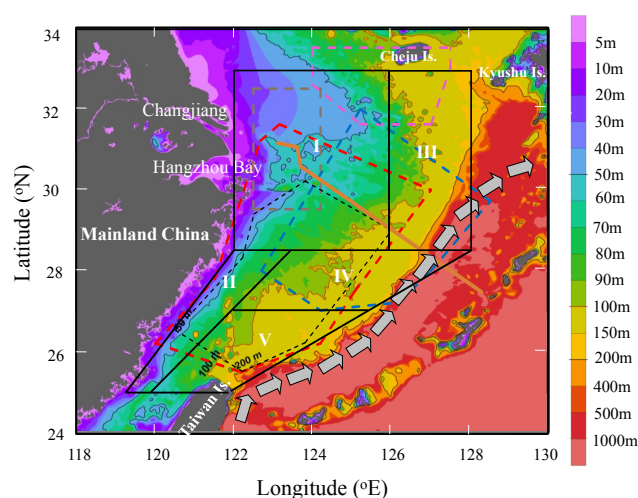

Figure 1. Map of the East China Sea showing the study area. Areas framed with black solid lines indicate the five physical–biogeochemical domains categorized in this study to better constrain the spatial and temporal variability in CO_2 fluxes, as detailed in Table 1. The arrows show the direction of the Kuroshio Current. Pink dashed lines indicate the study area of Shim et al. (2007) and Kim et al. (2013); brown dashed lines indicate that of Zhai and Dai (2009); blue dashed lines indicate that of Wang et al. (2000); red dashed lines indicate that of Chou et al. (2009; 2011) and Tseng et al. (2011); and black dashed lines indicate that of Peng et al. (1999). The solid brown line is the PN line, a regionally well-known transect from nearshore the Changjiang estuary to the southeastern Ryukyu Islands. Note that the colour bar for the depth scale is nonlinear.

the East Asian monsoon. The northeast winds in winter last from September to April, and the summer monsoon from the southwest is weaker and lasts from July to August. The Changjiang plume flows northeastward in summer but southwestward along the China coastline in winter (Lee and Chao, 2003). The northward-flowing Kuroshio follows the isobaths beyond the shelf break at ~ 200 m (Lee and Chao, 2003; Liu and Gan, 2012). Near the shelf break, there are upwellings centered on the northeast of Taiwan and the southwest of Kyushu Island (Lee and Chao, 2003).

The SST in the ECS is low in winter and early spring but high in summer and early autumn. The seasonal variation in SST is up to $10\,^{\circ}$C on the inner shelf and $\sim 5\,^{\circ}$C on the outer shelf (Gong et al., 2003). In warm seasons, productivity in the ECS is as high as > 1 g C m^{-2} d^{-1} (Gong et al., 2003). Changjiang freshwater and the upwelling of the Kuroshio subsurface water are believed to be the major sources of nutrients to the ECS shelf (Chen and Wang, 1999). Regulated by both productivity and temperature, pCO_2 shows strong seasonal variations, typically undersaturated in cold seasons and in productive areas in warm seasons (Chou et al., 2009; Chou et al., 2011; Tseng et al., 2011).

We categorized the ECS shelf into five distinct domains characterized by different physical–biogeochemical charac-

teristics based on the distributions of SST, chlorophyll *a* (Chl *a*) concentrations and turbidity (Fig. 1). The boundaries, surface areas and characteristics of the five domains are presented in Table 1 and Fig. 1. Domains I (28.5–33.0° N, 122.0–126.0° E; 191×10^3 km^2) and II (25.0–28.5° N, 119.3–123.5° E; 41×10^3 km^2) are essentially on the inner shelf shallower than 50 m. Domain I, being the core area of the outer Changjiang estuary and the near-field Changjiang plume in warm seasons, is characterized by high Chl *a* (He et al., 2013) and the lowest pCO$_2$ in warm seasons (Chen et al., 2008; Zhai and Dai, 2009). It covers most of the area within the 50 m isobaths. Domain II is off the Zhejiang–Fujian coast and characterized by turbid coastal waters and the Changjiang plume in winter. It has a strong seasonal variation in pCO$_2$. Domains III (28.5–33.0° N, 126.0–128.0° E; 96×10^3 km^2), IV (27.0–28.5° N, 123.5–128.0° E; 65×10^3 km^2) and V (25.0–27.0° N, 120.0–125.4° E; 60×10^3 km^2) are all located on the middle and outer shelf, influenced by the Kuroshio and thus characterized by lower nutrients and warm temperature. Domain III is located on the northern ECS shelf and generally dominated by temperature and impacted by the far-field Changjiang plume in flood seasons. Domain IV is located on the middle ECS shelf and is characterized by low Chl *a* all year round and high pCO$_2$ in warm seasons but is not impacted by the river plume (Bai et al., 2014). Domain V is on the southern ECS shelf where pCO$_2$ is dominated by temperature and may be under the influence of the northern Taiwan upwelling.

3   Materials and methods

3.1   Measurements of pCO$_2$, SST, SSS and auxiliary data

Twenty-four cruises and/or cruise legs were conducted from 2006 to 2011 in the ECS on board R/Vs *Dongfanghong II* and *Kexue III* and the fishing boat *Hubaoyu 2362*. Survey periods and areas are listed in Table 2. Sampling tracks are shown in Fig. 2. During the cruises, sea surface salinity (SSS), SST and pCO$_2$ were measured continuously. The methods of measurement and data processing followed those of Pierrot et al. (2009) and the SOCAT (Surface Ocean CO$_2$ Atlas, http://www.socat.info/news.html) protocol, which are briefly summarized here.

pCO$_2$ was continuously measured with a non-dispersive infrared spectrometer (Li-Cor®7000) integrated into a GO-8050 underway system (General Oceanic Inc. USA) on board *Dongfanghong II* or into a home-made underway system on board *Kexue III* and *Hubaoyu 2362*. The GO-8050 underway system is described by Pierrot et al. (2009). The home-made underway system is described by Zhai et al. (2007) and Zhai and Dai (2009); a Jiang et al. (2008) equilibrator was employed with this system. Surface water was continuously pumped from 1.5 to 5 m depth and measured every
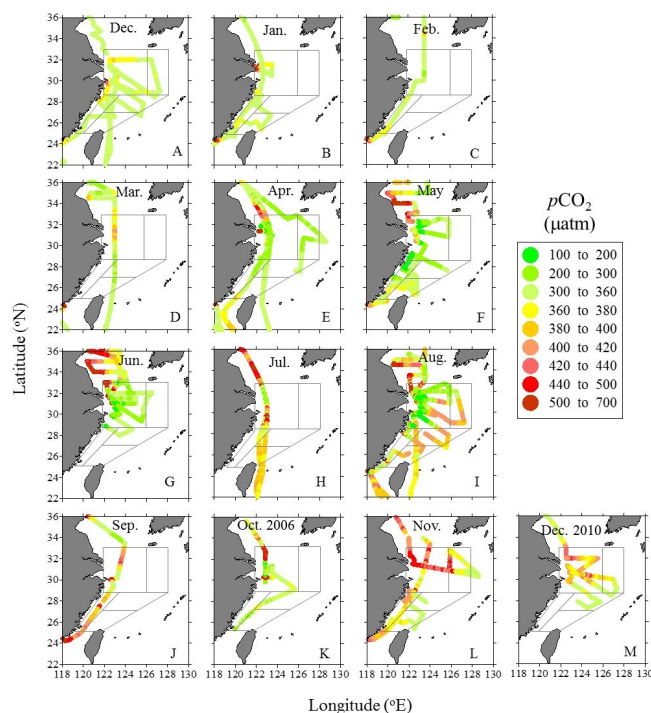

Figure 2. Monthly distribution of surface water pCO$_2$ (μatm) in the East China Sea based on the surveys from 2006 to 2011. The framed areas show the five physical–biogeochemical domains. Data are corrected to the reference year 2010.

80 s. CO$_2$ concentration in the atmosphere was determined every ~ 1.5 h. The bow intake for air sampling was installed ~ 10 m above the sea surface to avoid contamination from the ship. The barometric pressure was measured continuously onboard with a barometer attached at a level of ~ 10 m above the sea surface. The accuracy of the pCO$_2$ measurements was ~ 0.3 % (Zhai and Dai, 2009).

3.2   Data processing

Water pCO$_2$ at the temperature in the equilibrator (pCO$_2^{\text{Eq}}$) was calculated from the CO$_2$ concentration in the equilibrator (xCO$_2$) and the pressure in the equilibrator (P_{Eq}) after correction for the vapour pressure ($P_{\text{H}_2\text{O}}$) of water at 100 % relative humidity (Weiss and Price, 1980):

$$p\text{CO}_2^{\text{Eq}} = (P_{\text{Eq}} - P_{\text{H}_2\text{O}}) \times x\text{CO}_2. \tag{1}$$

pCO$_2$ in the air was calculated similarly using xCO$_2$ in the air and the barometric pressure. xCO$_2$ in the atmosphere over the Tae-ahn Peninsula (36.7376° N, 126.1328° E; Republic of Korea, http://www.esrl.noaa.gov/gmd/dv/site) was adopted in the atmospheric pCO$_2$ calculation after comparison with the field-measured values during the surveys.

Water pCO$_2^{\text{Eq}}$ obtained from Eq. (1) was corrected to pCO$_2$ at in situ temperature (in situ pCO$_2$, or hereafter pCO$_2$) using the empirical formula of Takahashi et

Table 1. Summary of the five physical–biogeochemical domains categorized in the East China Sea.

Domain	Location	Longitude (° E)	Latitude (° N)	Surface area (10^4 km^2)	Description and characteristics
I	Outer Changjiang Estuary and Changjiang plume	122–126	28.5–33	19.1	Lower estuary beyond the turbidity maximum zone and inner shelf influenced by river plume
II	Zhejiang–Fujian coast	119.33–123.5	25–28.5	4.1	Inner shelf dominated by turbid coastal waters with the influence of river plume primarily in winter
III	Northern East China Sea	126–128	28.5–33	9.6	Middle and outer shelf influenced by the Kuroshio; River plume signals visible in flood seasons
IV	Central East China Sea	122–128	27–28.5	6.5	Middle and outer shelf influenced by the Kuroshio
V	Southern East China Sea	120–125.42	25–27	6.0	Middle and outer shelf influenced by the Kuroshio and characterized by northern Taiwan upwelling

Table 2. Summary information of the 24 sampling surveys from 2006 to 2011.

Surveying time	Surveyed zones	Season	Sampling depth/RV	Sampler configuration	References/data source
1–3 January 2006	I	Winter	1.5 m (Fishing boat *Hubaoyu 2362*)	Modified from Jiang et al. (2008)	Zhai et al. (2007); Zhai and Dai (2009)
18–25 September 2006	I, II	Autumn	3 m (*Kexue 3*)	Modified from Jiang et al. (2008)	This study[a]
14–17 October 2006	I, II, IV	Autumn	3 m (*Kexue 3*)	Modified from Jiang et al. (2008)	This study[a]
20–24 November 2006	I, II	Autumn	5 m (*Dongfanghong 2*)	Modified from Jiang et al. (2008)	This study[a]
2–6 July 2007	I, II, V	Summer	5 m (*Dongfanghong 2*)	Modified from Jiang et al. (2008)	This study[a]
1–10 November 2007	I, III	Autumn	5 m (*Dongfanghong 2*)	GO8050	Zhai and Dai (2009)
20–30 April 2008	I, II	Spring	5 m (*Dongfanghong 2*)	GO8050	This study[a]
6–29 August 2008	I, II, IV, V	Summer	5 m (*Dongfanghong 2*)	GO8050	This study
23–31 December 2008	I, II. V	Winter	5 m (*Dongfanghong 2*)	GO8050	This study
10–14 January 2009	I, II	Winter	5 m (*Dongfanghong 2*)	GO8050	This study
15–27 March 2009	I, II, IV, V	Spring	5 m (*Dongfanghong 2*)	GO8050	This study
6–10 April 2009	I	Spring	1.5 m (*Hubaoyu 2362*)	Modified from Jiang et al. (2008)	This study
21–30 April 2009	I, II, III, IV, V	Spring	5 m (*Dongfanghong 2*)	GO8050	This study
1–13 May 2009	I, II, IV, V	Spring	5 m (*Dongfanghong 2*)	GO8050	This study
1–3 July 2009	I, II, IV, V	Summer	5 m (*Dongfanghong 2*)	GO8050	Wang et al. (2014)
17–31 August 2009	I, II, III, IV, V	Summer	5 m (*Dongfanghong 2*)	GO8050	Wang et al. (2014)
4–31 December 2009	I, II, III, IV, V	Winter	5 m (*Dongfanghong 2*)	GO8050	This study
1–5 January 2010	II, IV, V	Winter	5 m (*Dongfanghong 2*)	GO8050	This study
1–6 February 2010	I, II	Winter	5 m (*Dongfanghong 2*)	GO8050	This study
26–30 November 2010	II, IV, V	Autumn	5 m (*Dongfanghong 2*)	GO8050	This study
1–11 December 2010	I, III, IV	Winter	5 m (*Dongfanghong 2*)	GO8050	This study
13–15 April 2011	I, IV, V	Spring	5 m (*Dongfanghong 2*)	GO8050	This study
28–30 May 2011	II, III, IV, V	Spring	5 m (*Dongfanghong 2*)	GO8050	This study
1–8 June 2011	I, II, III, IV	Summer	5 m (*Dongfanghong 2*)	GO8050	This study

[a] Partially published in Zhai and Dai (2009).

al. (1993), where t is the temperature in the equilibrator.

$$\text{In situ } p\text{CO}_2 = p\text{CO}_2^{\text{Eq}} \times \exp((\text{SST-t}) \times 0.0423). \qquad (2)$$

Net CO$_2$ flux (F_{CO_2}) between the surface water and the atmosphere (or air–sea CO$_2$ flux) was calculated using the following formula:

$$F_{\text{CO}_2} = k \times s \times \Delta p\text{CO}_2, \qquad (3)$$

where s is the solubility of CO$_2$ (Weiss, 1974); $\Delta p\text{CO}_2$ is the $p\text{CO}_2$ difference between the surface water and the atmosphere; and k is the CO$_2$ transfer velocity. k was parameterized using the empirical function of Sweeney et al. (2007), and the nonlinear correction of gas transfer velocity with wind speed was adopted following Wanninkhof et al. (2002)

and Jiang et al. (2008):

$$k(\text{S07}) = 0.27 \times \text{C}_2 \times U_{\text{mean}}^2 \times (Sc/660)^{-0.5} \qquad (4)$$

$$\text{C}_2 = \left(\frac{1}{n} \sum_{j=1}^{n} U_j^2 \right) U_{\text{mean}}^2, \qquad (5)$$

where U_{mean} is the monthly mean wind speed at 10 m above the sea level (in m s^{-1}) and Sc is the Schmidt number at in situ temperature of surface seawater (Wanninkhof, 1992). C$_2$ is the nonlinear coefficient for the quadratic term of the gas transfer relationship; U_j is the high-frequency wind speed (in m s^{-1}); the subscript "mean" indicates the average; and n is the number of available wind speeds in a month. Wind speeds at a spatial resolution of 1° × 1° and temporal resolution of 6 h were obtained from the US National Centers for Environmental Prediction (NCEP, http://oceandata.sci.gsfc. nasa.gov/Ancillary/Meterological), and the monthly average
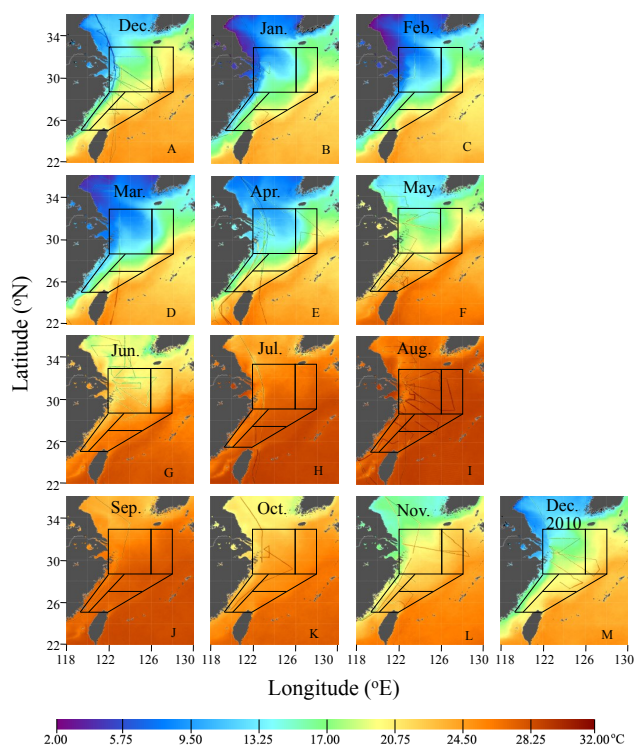
Figure 3. Monthly distribution of sea surface temperature (SST) in the East China Sea during the surveys from 2006 to 2011. The climatology (from 2003 to 2013) monthly mean SST were calculated based on the monthly mean SST obtained from the NASA ocean colour website (http://oceancolor.gsfc.nasa.gov), which were retrieved with the Moderate Resolution Imaging Spectroradiometer (MODIS) on board the Aqua satellite. The 4 μm nighttime SST products were used here. The SST data in the track were measured during the surveys. The framed areas show the five physical–biogeochemical domains. In panel (**m**), the SST data in the track were measured during the December 2010 cruise, while the background is the climatology (from 2003 to 2013) monthly mean SST.

Figure 4. Seasonal variations in sea surface temperature (SST, **a**) and salinity (SSS, **b**) in Domain I (red curve), Domain II (blue curve), Domain III (pink curve), Domain IV (green curve) and Domain V (black curve). The mean SST data were retrieved with the Moderate Resolution Imaging Spectroradiometer (MODIS) on board the Aqua satellite from the NASA ocean colour website (http://oceancolor.gsfc.nasa.gov). The 4 μm nighttime SST products were used here. The mean SSS were based on the data presented in Tables 3–7. The data from each survey are shown as mean ± standard deviation.

was adopted in the CO$_2$ flux calculations. As defined here, a positive flux indicates an evasion of CO$_2$ from the sea to the air.

The seasonal amplitude and spatial variation in SST in the ECS are large, up to $> 10\,°C$, which significantly impacts the pCO$_2$. To distinguish the influence of biogeochemical processes from the thermodynamics effect, pCO$_2$ was normalized to a constant temperature following Takahashi et al. (2002) and termed NpCO$_2$:

$$\text{N}p\text{CO}_2 = p\text{CO}_2 \times \exp(0.0423 \times (21 - \text{SST})). \tag{6}$$

Here, $21\,°C$ was used since it corresponded to the average SST during the cruises.

Our surveys covered the four seasons of the year, among which we defined March to May as spring, June to August as summer, September to November as autumn and December to February as winter.
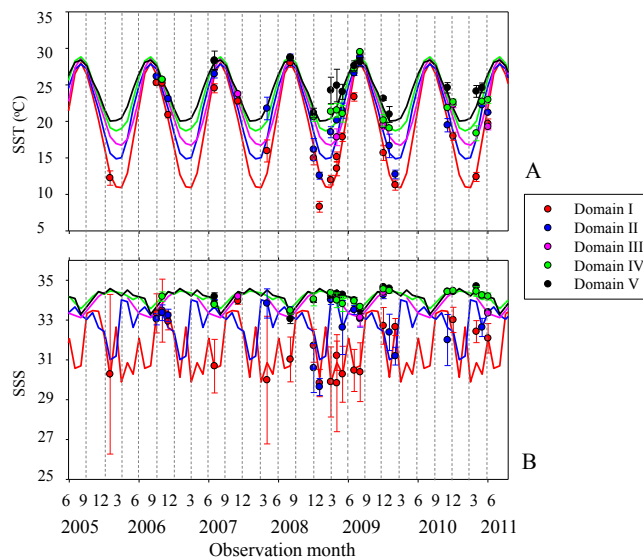
On a global scale, both the atmospheric pCO$_2$ and the surface seawater pCO$_2$ are increasing and the rate of increase differs in different regions (Takahashi et al., 2009). Tseng et al. (2014) report that the increasing rate of pCO$_2$ is 1.9 and 2.1 μatm yr^{-1} for the atmosphere and the surface seawater, respectively, in the ECS based on the observations from 1998 to 2012. We assumed that these yearly change rates were evenly distributed across the months; based on this assumption we corrected the pCO$_2$ data to June 2010.

4 Results

4.1 SST and SSS

Figure 3 reveals strong temporal and spatial variations in SST over the 12 months of the year. The seasonal variation in the average SST and SSS in the five domains is further shown in Fig. 4 and Tables 3 to 7. In winter and spring, SST increased offshore and from north to south with a range of ~ 8 to $25\,°C$, and the highest SST appeared in the southeastern part of the ECS. In summer and autumn, SST was high and relatively spatially homogeneous compared to that in winter and spring with a range of ~ 18 to $30\,°C$. On a monthly timescale, the lowest SSTs appeared in January to March and the highest in July to September (Fig. 3). The magni-

tude of seasonal variation in SST decreased offshore, from 12 to 14 °C in Domains I and II to 6 to 8 °C in Domains IV and V. The lowest SST was observed in Domain I in January 2009 and was 8.1 ± 0.8 °C (Fig. 4). In July and August, there was a northeastern-oriented filament with relatively low SST off eastern Taiwan (Fig. 3). The average SST measured underway during the surveys in the entire study area was 17.8 ± 2.2 °C in winter, 19.7 ± 2.9 in spring, 26.2 ± 1.8 in summer and 23.2 ± 1.2 °C in autumn.

Spatially, salinity increased offshore and the highest salinity appeared in the area affected by the Kuroshio (not shown). On the whole-shelf scale, the lowest salinity was observed in Domain I, where it was lower in March to August (29 to 32) and higher in September to February (30 to 34). The low SSS in spring and summer corresponded to the high freshwater discharge of the year from the Changjiang. SSS in June was relatively high compared to that in March, April, May, July and August (Fig. 4b), which might be attributed to the fact that there was only one June survey (June 2011) and this survey followed an exceptionally dry May. The discharge of the Changjiang in May of 2011 was ~ 40 % lower than the monthly average of 2005 to 2011 (data at Datong gauge station, the Hydrological Information Annual Report 2005 to 2011, Ministry of Water Resources, P. R. China). On a seasonal scale, the average SSS in Domain I was lowest in spring (30.6 ± 4.6) and summer (30.9 ± 1.4) and highest in autumn (33.4 ± 0.9). SSS in winter (31.5 ± 2.3) was higher than in spring to summer but lower than in autumn. The seasonality of SSS in Domain II was different from that of Domain I (Table 3), and was lower in November to February (29.6 to 34.3) than in March to October (32.6 to 34.0, Fig. 4b). This seasonality might be attributed to the fact that the Changjiang plume and coastal current were southwestward in winter (Han et al., 2013; Lee and Chao, 2003). The seasonal variation in SSS in Domains I and II was up to 2.7 to 2.8.

Data in Domain III were rather limited, but SSS in winter (34.4 ± 0.2) and autumn (34.2 ± 0.1) was higher than that in summer (33.1 ± 0.6; Table 5). The seasonality of SSS in Domains IV and V was similar, showing low SSS in July to September (33 to 34) but high SSS in other months (> 34). Seasonal variation in SSS in these two domains was < 1, which was much smaller than that in Domains I, II and III. The average salinity in the entire study area was 33.2 ± 2.5 in winter, 33.3 ± 4.7 in spring, 33.0 ± 1.6 in summer and 33.8 ± 1.3 in autumn.

4.2 Wind speeds and C_2

The temporal patterns of the wind speeds in the five domains were similar (Tables 3 to 7). The monthly average wind speeds ranged from 5.3 to 11.4 m s^{-1} and their standard deviations (SDs) were lower than 1 m s^{-1}. Generally, wind speed was high in autumn and winter but low in spring and summer with large interannual variations. The highest wind speeds were recorded in Domains II, IV and V in November

2007, when the monthly average wind speeds reached 10.4 to 11.4 m s^{-1}. The lowest wind speeds were observed in August 2008, May 2009 and May 2011, when the monthly average wind speeds ranged from 5.6 to 6.5 m s^{-1}. Wind speeds in September, October and November 2006 were relatively low compared to other autumn months and, in March 2009, were relatively high compared to other spring months.

C_2 ranged from 1.06 to 1.70 and the annual average C_2 in the five domains was 1.21 ± 0.04, 1.20 ± 0.09, 1.21 ± 0.06, 1.19 ± 0.08 and 1.19 ± 0.13, which was similar to or slightly lower than the global average of 1.27 (Wanninkhof et al., 2009).

4.3 CO_2 concentration in the air

Field-observed CO_2 concentrations in the air over the ECS ranged 370 to 410 µatm, which was not inconsistent with the global increase in atmospheric pCO_2. Both the seasonal and interannual patterns we measured during the surveys were similar to those observed at the Tae-ahn Peninsula (Korea-China Center for Atmospheric Research, Republic of Korea), with the highest values typically observed in February to April and the lowest values in July to September (Fig. 5). The difference in atmospheric CO_2 between our shipboard measurements over the ECS and that observed at the Tae-ahn Peninsula was not significant, ranging from 0.1 to 7.9 ppm (average ~ 3.5 ppm). However, the amplitude of the seasonal variation in air CO_2 concentration over the ECS was larger than that over the open North Pacific (Mauna Loa station), which was 5 to 10 ppm. Both the air CO_2 concentration over the ECS and the Tae-ahn Peninsula were higher than that at the Mauna Loa station, which might be due to the fact that the marine boundary atmosphere over marginal seas has more impacts from terrestrial sources.

4.4 Surface seawater pCO_2

pCO_2 values along the cruise tracks in this study are shown in Fig. 2. By averaging the pCO_2 values on these tracks to $1° \times 1°$ grids, we obtained the mean pCO_2 values in the five domains (Tables 3 to 7).

For the entire ECS shelf, pCO_2 was relatively homogeneous in winter, but strong spatial variations occurred in other seasons (Fig. 2). In Domain I, pCO_2 was generally low (< 360 µatm) in winter, spring and summer except in the area off the Changjiang estuary mouth and in Hangzhou Bay and the northwestern corner, which may be influenced by the southern Yellow Sea through the Yellow Sea Coastal Current (Su, 1998) that carried higher CO_2 water southward. However, in autumn, pCO_2 was generally high (> 380 µatm) except in October 2006. In Domain II, both the seasonal evolution and the pCO_2 values were generally overall similar to those of Domain I, but pCO_2 in summer was higher than in Domain I based on the limited data available (Fig. 2). In Domains I and II, the seasonal average pCO_2 values were 348

Table 3. Data summary of Domain I. "Atm. pCO$_2$" is atmospheric pCO$_2$; SST is sea surface temperature; SSS is sea surface salinity; F_{CO_2} is the air–sea CO$_2$ flux; and SD is standard deviation. C$_2$ is the nonlinearity effect of the short-term variability in wind speeds over 1 month on the gas transfer velocity, assuming that long-term winds followed a Raleigh (Weibull) distribution (Wanninkhof, 1992; Jiang et al., 2008). See text for details. October 2006 and December 2010 were excluded in the calculations of seasonal averages. pCO$_2$ data are corrected to the reference year 2010.

Season	Period	pCO$_2$ (µatm)		Atm. pCO$_2$ (µatm)		ΔpCO$_2$ (µatm)		SST (°C)		SSS		Wind speed (m s^{-1})		C$_2$	FCO$_2$ (mmol m^{-2} d^{-1})	
		Mean	SD	Mean	SD	Mean	SD	Mean	SD	Mean	SD	Mean	SD		Mean	SD
Winter	23–31 December 2008	356.4	7.2	392.2	0.3	−35.8	7.2	15.0	0.9	31.71	0.86	8.05	0.63	1.24	−7.9	2.2
	4–31 December 2009	352.6	9.3	389.4	0.6	−36.8	9.3	15.7	1.1	32.71	0.96	8.24	0.91	1.19	−7.7	4.0
	1–3 January 2006	360.7	17.5	395.4	1.6	−34.7	17.5	12.2	1.1	30.28	4.28	8.12	0.82	1.14	−6.5	6.9
	1–14 January 2009	341.4	2.6	399.3	0.4	−58.0	2.6	8.1	0.8	29.98	0.73	8.42	0.89	1.20	−13.5	1.9
	1–5 January 2010	–	–	–	–	–	–	–	–	–	–	7.95	0.85	1.22	–	–
	1–6 February 2010	329.8	6.6	395.7	0.2	−65.9	6.6	11.3	0.7	32.65	0.45	7.86	0.72	1.21	−13.3	3.8
	1–11 December 2010	384.2	19.7	390.3	0.5	−6.1	19.7	18.0	0.6	33.01	0.65	9.11	0.67	1.23	−1.6	7.5
	Seasonal average	348.2	11.1	394.4	0.9	−46.2	11.1	12.4	1.0	31.47	2.28	8.11	0.89	1.20	−9.8	4.7
Spring	15–27 March 2009	359.4	13.4	391.9	0.4	−32.5	13.5	12.0	0.7	29.89	1.97	7.68	0.93	1.16	−5.8	6.2
	20–30 April 2008	315.6	53.0	396.5	0.7	−81.0	53.0	16.0	1.7	29.99	7.03	5.83	0.41	1.27	−9.9	6.0
	21–30 April 2009	303.5	28.2	395.9	0.3	−92.3	28.2	15.1	0.8	31.21	0.79	5.94	0.42	1.26	−11.5	4.6
	6–10 April 2009	286.3	101.7	398.6	0.7	−112.3	101.7	13.5	1.1	29.83	6.85	5.94	0.42	1.26	−14.0	11.1
	12–15 April 2011	295.8	46.0	398.9	0.4	−103.1	46.0	12.4	0.7	32.42	0.62	6.25	0.31	1.25	−14.0	8.8
	1–20 May 2009	292.7	41.2	388.3	0.4	−95.6	41.2	17.8	0.6	30.28	1.45	5.43	0.26	1.20	−8.9	6.3
	26–31 May 2011	–	–	–	–	–	–	–	–	–	–	5.79	0.23	1.21	–	–
	Seasonal average	308.9	59.9	395.0	0.5	−86.1	59.9	14.5	1.1	30.60	4.55	6.12	0.52	1.23	−10.7	8.2
Summer	1–12 July 2009	357.2	56.0	369.5	0.6	−12.3	56.0	23.3	0.6	30.47	1.18	6.40	0.52	1.18	−1.6	9.3
	2–6 July 2007	292.7	56.1	374.9	0.5	−82.1	56.1	24.5	0.7	30.69	1.50	5.57	0.77	1.27	−8.9	7.3
	6–29 August 2008	339.8	77.9	374.6	0.5	−34.8	77.9	28.0	0.6	31.02	1.16	5.41	0.50	1.21	−3.3	12.6
	17–31 August 2009	293.8	64.5	362.8	0.6	−69.0	64.5	28.6	0.7	30.38	1.52	6.13	0.32	1.22	−8.4	9.7
	1–19 June 2011	302.4	64.6	387.6	0.7	−85.2	64.6	19.7	0.7	32.08	0.76	5.85	0.49	1.27	−10.2	8.0
	Seasonal average	317.2	71.9	373.9	0.6	−56.7	71.9	24.8	0.7	30.93	1.41	5.87	0.60	1.23	−6.5	10.7
Autumn	18–25 September 2006	387.8	50.0	374.9	0.7	12.9	50.0	25.3	0.3	33.34	1.08	7.01	0.56	1.19	2.7	5.8
	14–18 October 2006	364.3	65.6	382.8	0.4	−18.5	65.6	25.2	0.4	33.47	1.67	6.12	0.61	1.13	−1.9	5.5
	20–24 November 2006	396.9	23.6	386.3	0.3	10.6	23.6	20.9	0.4	32.93	0.46	7.74	0.69	1.17	1.9	3.7
	1–10 November 2007	395.7	14.4	385.5	0.3	10.3	14.4	22.7	0.3	33.95	0.17	8.14	1.06	1.13	1.9	6.8
	26–30 November 2010	–	–	–	–	–	–	–	–	–	–	6.73	0.74	1.22	–	–
	Seasonal average	393.5	40.4	382.2	0.6	11.3	40.4	23.0	0.5	33.41	0.84	7.41	0.91	1.17	2.2	6.8
Annual average		341.9	59.2	386.4	0.8	−44.4	59.2	18.7	1.0	31.60	3.08	6.88	0.86	1.21	−6.2	9.1

and 349 µatm in winter, 309 and 313 µatm in spring, 317 and 357 µatm in summer, and 393 and 388 µatm in autumn (Tables 3 and 4). The seasonal pattern in Domains IV and V was different, showing relatively low pCO$_2$ (< 360 µatm) in winter, spring and autumn but high pCO$_2$ (> 370 µatm) in summer (Fig. 2). The seasonal average pCO$_2$ values in these two domains were 341 and 344 µatm in winter, 318 and 345 µatm in spring, 380 and 381 µatm in summer and 336 and 348 µatm in autumn (Tables 6 and 7). Temporal coverage was sparse in Domain III. Based on the limited data available, the seasonality of pCO$_2$ in Domain III was similar to those of Domains IV and V (Table 5). The seasonal variation was largest in Domains I, II and III (~ 80 to 90 µatm) and smallest in Domain V (37 µatm).

In addition to the strong seasonal variation, intra-seasonal variability was also substantial. In Domain I, the intra-seasonal variation in pCO$_2$ was ~ 30 to 73 µatm during the winter, spring and summer cruises but relatively smaller in autumn (< 10 µatm excluding the October 2006 and December 2010 surveys; Table 3). In Domain II, it was much

smaller in winter (< 10 µatm) than in other seasons (30 to 80 µatm; Table 4). In Domains IV and V, it was ~ 10 µatm in winter, but relatively higher variability occurred in spring and summer (14 to 55 µatm; Tables 6 and 7).

Based on the seasonal average as shown in Fig. 6, the overall characteristics of the pCO$_2$ distribution were conspicuous. In winter, the pCO$_2$ was relatively homogeneous and the average pCO$_2$ in each domain ranged from 340 to 349 µatm. In spring, the gridded pCO$_2$ values were lower than those in winter except in the northwest corner and the area near the Changjiang estuary. The seasonal average pCO$_2$ values in the domains were generally lower than in winter (309 ± 60, 313 ± 24, 290 ± 10, 318 ± 17 and 345 ± 12 µatm in the five domains) since the high pCO$_2$ values were located in very limited grids. In summer, pCO$_2$ was lower on the inner shelf and higher on the outer shelf with extremely high pCO$_2$ in the northwest corner and off the Changjiang estuary mouth and Hangzhou Bay. The seasonal average pCO$_2$ was 317 ± 72, 357 ± 22, 341 ± 18, 380 ± 9.0 and 381 ± 16 µatm in the five domains. In autumn, the average pCO$_2$ was

Table 4. Data summary of Domain II. "Atm. pCO$_2$" is atmospheric pCO$_2$; SST is sea surface temperature; SSS is sea surface salinity; F_{CO_2} is the air–sea CO$_2$ flux; and SD is standard deviation. C$_2$ is the nonlinearity effect of the short-term variability in wind speeds over 1 month on the gas transfer velocity, assuming that long-term winds followed a Raleigh (Weibull) distribution (Wanninkhof, 1992; Jiang et al., 2008). See text for details. October 2006 and December 2010 were excluded in the calculations of seasonal averages. pCO$_2$ data are corrected to the reference year 2010.

Season	Period	pCO$_2$ (µatm)		Atm. pCO$_2$ (µatm)		ΔpCO$_2$ (µatm)		SST (°C)		SSS		Wind speed (m s^{-1})		C$_2$	F_{CO_2} (mmol m^{-2} d^{-1})	
		Mean	SD	Mean	SD	Mean	SD	Mean	SD	Mean	SD	Mean	SD		Mean	SD
Winter	23–31 December 2008	350.3	8.0	389.0	0.9	−38.6	8.1	16.2	1.7	30.59	1.38	8.56	0.99	1.18	−8.7	1.4
	4–31 December 2009	343.8	7.7	389.8	0.6	−46.1	7.7	19.4	0.7	34.26	0.26	8.02	0.74	1.17	−8.7	0.3
	1–3 January 2006	–	–	–	–	–	–	–	–	–	–	8.71	0.88	1.11	–	–
	1–14 January 2009	347.7	4.5	395.0	0.3	−47.3	4.5	12.7	0.5	29.64	0.47	9.01	1.02	1.12	−10.9	0.9
	1–5 January 2010	353.0	9.3	391.4	1.5	−38.4	9.4	16.6	1.6	32.38	0.91	7.90	0.76	1.22	−7.8	1.9
	1–6 February 2010	352.4	7.2	392.5	0.5	−40.1	7.2	12.7	0.7	31.19	0.49	7.98	0.59	1.20	−8.3	1.6
	1–11 December 2010	–	–	–	–	–	–	–	–	–	–	7.83	0.71	1.28	–	–
	Seasonal average	349.4	8.4	391.5	1.0	−42.1	8.4	15.5	1.3	31.61	0.90	8.36	0.92	1.18	−8.9	1.4
Spring	15–27 March 2009	308.5	13.4	389.6	0.5	−81.1	13.4	18.5	0.8	34.01	0.23	8.30	0.69	1.14	−15.7	2.6
	20–30 April 2008	331.2	22.5	392.0	1.1	−60.9	22.6	21.8	1.7	33.83	0.82	6.38	0.53	1.19	−7.5	3.3
	21–30 April 2009	312.4	11.7	392.1	0.3	−79.7	11.7	20.1	0.2	34.01	0.06	7.00	0.97	1.17	−11.5	1.7
	6–10 April 2009	–	–	–	–	–	–	–	–	–	–	7.00	0.97	1.17	–	–
	12–15 April 2011	–	–	–	–	–	–	–	–	–	–	6.57	0.52	1.24	–	–
	1–20 May 2009	290.6	35.8	386.7	0.7	−96.1	35.8	21.5	1.1	32.63	1.47	5.67	0.56	1.18	−9.4	4.0
	26–31 May 2011	323.1	11.9	394.8	0.9	−71.7	11.9	22.2	0.2	32.63	0.56	6.26	0.42	1.23	−9.1	3.4
	Seasonal average	313.2	23.7	391.1	0.8	−77.9	23.7	20.8	1.1	33.42	0.89	6.74	0.75	1.19	−10.7	3.5
Summer	1–12 July 2009	361.4	16.9	367.1	0.4	−5.7	16.9	26.6	0.3	33.51	0.22	6.33	0.51	1.19	−0.7	2.0
	2–6 July 2007	346.9	11.8	373.5	0.4	−26.6	11.8	26.5	0.8	33.81	0.31	6.86	0.59	1.21	−3.9	1.6
	6–29 August 2008	397.3	2.9	374.7	0.3	22.6	2.9	28.8	0.5	33.40	0.28	5.56	0.40	1.23	2.3	0.3
	17–31 August 2009	363.3	38.0	362.8	0.3	0.5	38.0	28.8	0.3	33.06	0.47	6.19	0.27	1.52	0.1	6.0
	1–19 June 2011	318.6	0.3	387.7	1.6	−69.1	1.6	21.2	0.0	33.40	0.02	6.78	0.43	1.18	−9.5	0.0
	Seasonal average	357.5	21.7	373.2	0.9	−15.7	21.7	26.4	0.5	33.44	0.33	6.34	0.51	1.27	−2.4	3.3
Autumn	18–25 September 2006	407.5	14.2	374.8	0.6	32.8	14.2	26.1	0.1	33.04	0.31	7.28	0.77	1.19	5.2	3.0
	14–18 October 2006	308.4	25.3	381.6	0.2	−73.3	25.3	25.7	0.1	33.37	0.43	7.17	1.07	1.12	−10.1	4.7
	20–24 November 2006	377.7	8.1	377.7	8.1	0.0	11.4	23.1	0.3	33.23	0.34	6.97	0.75	1.18	−1.0	1.2
	1–10 November 2007	–	–	–	–	–	–	–	–	–	–	10.81	1.40	1.07	–	–
	26–30 November 2010	378.5	16.4	388.5	0.6	−10.1	16.5	19.5	1.0	32.00	1.40	9.01	1.29	1.10	−2.1	4.8
	Seasonal average	387.9	16.4	380.3	5.7	7.6	17.4	22.9	0.8	32.76	1.05	8.52	1.26	1.13	0.7	4.1
Annual average		352.0	21.4	384.0	3.4	−32.0	21.6	21.4	1.1	32.81	0.97	7.49	1.04	1.19	−5.3	3.7

393 ± 40 µatm in Domain I, which was significantly higher than in the offshore domains (336 to 367 µatm).

It is worth noting that the two cruises conducted in October 2006 and December 2010 appeared to be atypical. The results of these two cruises were significantly different from other surveys in the respective seasons. In the October 2006 cruise, the pCO$_2$ went down to 364 µatm in Domain I and 308 µatm in Domain II, which was 29 and 80 µatm lower than the averages of other autumn cruises in the two domains. In the December 2010 cruise, pCO$_2$ in Domain I was as high as 384 µatm, which was 36 µatm higher than the average pCO$_2$ of the other winter cruises (Fig. 6). We will further discuss these cruises in the Discussion section.

The distribution of the SD of pCO$_2$ showed strong spatial and seasonal variations with a large range of 1 to 185 µatm (Fig. 6). In Domain I, the SD was low in winter and high in spring and summer. The highest SD occurred in summer in the coastal area off the Changjiang estuary mouth and in Hangzhou Bay with the highest value of 80 to 185 µatm. The SD in Domain II ranged from 1 to 48 µatm, with higher val-

ues in spring and summer. In Domain III, the range of SD was 1 to 19 µatm and showed no remarkable seasonal pattern. In Domains IV and V, the SD range was 1 to 29 µatm with relatively higher values in spring and autumn but lower values in winter and summer in Domain IV and higher ones in spring and summer but lower ones in autumn and winter in Domain V. Since pCO$_2$ distribution was generally homogeneous in winter except in December 2010, the SD in winter was relatively low, as expected, and in > 85 % of grids it was < 10 µatm, and the highest SD was 17 µatm. The SD in October 2006 in Domain I was higher than in the other autumn surveys and the SD in Domain I in December 2010 was higher than in the other winter surveys.

It should be noted that the SD of pCO$_2$ represents the mixture of sources of uncertainty in the gridded pCO$_2$ data, the analytical error, the spatial variance, and the bias from undersampling. Wang et al. (2014) demonstrate that the analytical errors are almost the same on the ECS shelf and the latitudinal distribution of SD is similar to that of the spatial variance. Thus, higher SD usually reflects higher spatial variance and

Table 5. Data summary of Domain III. "Atm. pCO$_2$" is atmospheric pCO$_2$; SST is sea surface temperature; SSS is sea surface salinity; F_{CO_2} is the air–sea CO$_2$ flux; and SD is standard deviation. C$_2$ is the nonlinearity effect of the short-term variability in wind speeds over 1 month on the gas transfer velocity, assuming that long-term winds followed a Raleigh (Weibull) distribution (Wanninkhof, 1992; Jiang et al., 2008). See text for details. October 2006 and December 2010 were excluded in the calculations of seasonal averages. pCO$_2$ data are corrected to the reference year 2010.

Season	Period	pCO$_2$ (µatm)		Atm. pCO$_2$ (µatm)		ΔpCO$_2$ (µatm)		SST (°C)		SSS		Wind speed (m s^{-1})		C$_2$	F_{CO_2} (mmol m^{-2} d^{-1})	
		Mean	SD	Mean	SD	Mean	SD	Mean	SD	Mean	SD	Mean	SD		Mean	SD
Winter	23–31 December 2008	–	–	–	–	–	–	–	–	–	–	8.21	0.16	1.25	–	–
	4–31 December 2009	340.1	8.8	385.9	0.5	−45.7	8.8	19.6	0.8	34.38	0.15	8.86	0.30	1.18	−10.8	1.4
	1–3 January 2006	–	–	–	–	–	–	–	–	–	–	8.79	0.38	1.13	–	–
	1–14 January 2009	–	–	–	–	–	–	–	–	–	–	9.21	0.25	1.18	–	–
	1–5 January 2010	–	–	–	–	–	–	–	–	–	–	8.48	0.36	1.21	–	–
	1–6 February 2010	–	–	–	–	–	–	–	–	–	–	8.39	0.31	1.19	–	–
	1–11 December 2010	335.2	9.2	387.3	0.5	−52.2	9.2	22.3	0.5	34.42	0.04	9.79	0.51	1.20	−15.3	5.2
	Seasonal average	340.1	8.8	385.9	0.5	−45.7	8.8	19.6	0.8	34.38	0.15	8.66	0.30	1.19	−10.8	1.4
Spring	15–27 March 2009	–	–	–	–	–	–	–	–	–	–	8.81	0.36	1.13	–	–
	20–30 April 2008	–	–	–	–	–	–	–	–	–	–	6.68	0.38	1.21	–	–
	21–30 April 2009	289.5	10.4	396.2	0.8	−106.7	10.4	17.8	1.2	34.14	0.27	6.95	0.62	1.26	−17.8	3.1
	6–10 April 2009	–	–	–	–	–	–	–	–	–	–	6.95	0.62	1.26	–	–
	12–15 April 2011	–	–	–	–	–	–	–	–	–	–	6.93	0.27	1.24	–	–
	1–20 May 2009	–	–	–	–	–	–	–	–	–	–	6.17	0.41	1.20	–	–
	26–31 May 2011	–	–	–	–	–	–	–	–	–	–	5.61	0.25	1.25	–	–
	Seasonal average	289.5	10.4	396.2	0.8	−106.7	10.4	17.8	1.2	34.14	0.27	6.87	0.62	1.22	−17.8	3.1
Summer	1–12 July 2009	–	–	–	–	–	–	–	–	–	–	6.69	0.23	1.14	–	–
	2–6 July 2007	–	–	–	–	–	–	–	–	–	–	5.94	0.61	1.40	–	–
	6–29 August 2008	–	–	–	–	–	–	–	–	–	–	6.23	0.39	1.18	–	–
	17–31 August 2009	378.3	10.2	362.1	0.3	16.2	10.2	29.4	0.3	33.12	0.49	5.59	0.25	1.28	1.8	3.7
	1–19 June 2011	304.0	14.5	386.6	1.2	−82.6	14.5	19.3	0.8	33.34	0.35	6.10	0.65	1.28	−10.9	1.6
	Seasonal average	341.1	17.7	374.3	1.2	−33.2	17.8	24.3	0.9	33.23	0.60	6.11	0.52	1.26	−4.6	4.0
Autumn	18–25 September 2006	–	–	–	–	–	–	–	–	–	–	7.08	0.88	1.20	–	–
	14–18 October 2006	–	–	–	–	–	–	–	–	–	–	7.03	0.59	1.14	–	–
	20–24 November 2006	–	–	–	–	–	–	–	–	–	–	7.82	0.52	1.17	–	–
	1–10 November 2007	367.3	8.6	384.9	0.3	−17.6	8.6	23.7	0.3	34.19	0.06	8.96	0.50	1.11	−3.7	5.1
	26–30 November 2010	–	–	–	–	–	–	–	–	–	–	7.40	0.20	1.17	–	–
	Seasonal average	367.3	8.6	384.9	0.3	−17.6	8.6	23.7	0.3	34.19	0.06	7.82	0.50	1.16	−3.7	5.1
Annual average		334.5	13.8	385.3	0.9	−50.8	13.8	21.4	1.0	33.98	0.39	7.36	0.57	1.21	−9.2	4.2

vice versa along latitudes. However, the SD was equivalent to neither the spatial variance nor the bulk uncertainty and the bias from undersampling may exert the greatest uncertainty in the gridded pCO$_2$ in grids with poor sampling coverage (Wang et al., 2014).

4.5 Air–sea CO$_2$ fluxes

Similar to the different seasonality of pCO$_2$ in the differing domains, the air–sea CO$_2$ fluxes also had strong seasonal variations in each domain and the seasonal pattern differed among the domains (Tables 3 to 7).

Domain I was a sink of atmospheric CO$_2$ during all the winter, spring and summer surveys, with CO$_2$ fluxes ranging from −14.0 to −1.6 mmol m^{-2} d^{-1}. However, Domain I in autumn was a weak source of 2.2 ± 6.8 mmol m^{-2} d^{-1}, with a flux range of 1.9 to 2.7 mmol m^{-2} d^{-1} (Table 3). The CO$_2$ fluxes we estimated were similar to those estimated by Zhai and Dai (2009) based on multiple observations (-10.4 ± 2.3,

-8.8 ± 5.8, -4.9 ± 4.0 and 2.9 ± 2.9 mmol m^{-2} d^{-1} in winter, spring, summer and autumn, respectively).

Similar to Domain I, Domain II was also a strong sink in winter and spring with a CO$_2$ flux range of −15.7 to −7.5 mmol m^{-2} d^{-1}. The seasonal average flux was -8.9 ± 1.4 in winter and -10.7 ± 3.5 mmol m^{-2} d^{-1} in spring. The sink weakened in summer and the seasonal average CO$_2$ flux was -2.4 ± 3.3 mmol m^{-2} d^{-1}. In autumn, Domain II was a CO$_2$ source of 0.7 ± 4.1 mmol m^{-2} d^{-1} (Table 4).

Although considerable variability occurred, Domains III, IV and V were generally strong sinks in winter, spring and autumn (−3.7 to −18.7 mmol m^{-2} d^{-1}) but weak to moderate sources in summer (0 to 6.8 mmol m^{-2} d^{-1}, except in June 2011 when it was a strong sink). On a seasonal timescale, CO$_2$ fluxes in Domains III, IV and V ranged from −10.0 to −10.8 in winter, −6.8 to −17.8 in spring, −3.7 to −9.3 in autumn, and 1.0 to 1.8 mmol m^{-2} d^{-1} in summer (Tables 5, 6 and 7).

Table 6. Data summary of Domain IV. "Atm. pCO_2" is atmospheric pCO_2; SST is sea surface temperature; SSS is sea surface salinity; F_{CO_2} is the air–sea CO_2 flux; and SD is standard deviation. C_2 is the nonlinearity effect of the short-term variability in wind speeds over 1 month on the gas transfer velocity, assuming that long-term winds followed a Raleigh (Weibull) distribution (Wanninkhof, 1992; Jiang et al., 2008). See text for details. October 2006 and December 2010 were excluded in the calculations of seasonal averages. pCO_2 data are corrected to the reference year 2010.

Season	Period	pCO_2 (µatm)		Atm. pCO_2 (µatm)		ΔpCO_2 (µatm)		SST (°C)		SSS		Wind speed (m s^{-1})		C_2	F_{CO_2} (mmol m^{-2} d^{-1})	
		Mean	SD	Mean	SD	Mean	SD	Mean	SD	Mean	SD	Mean	SD		Mean	SD
Winter	23–31 December 2008	335.5	3.8	387.5	0.3	−52.0	3.8	20.6	0.6	34.04	0.32	8.85	0.34	1.16	−11.8	0.9
	4–31 December 2009	339.1	5.1	387.3	0.7	−48.2	5.1	20.1	0.8	34.55	0.08	8.60	0.19	1.19	−10.8	1.6
	1–3 January 2006	–	–	–	–	–	–	–	–	–	–	9.02	0.30	1.11	–	–
	1–14 January 2009	–	–	–	–	–	–	–	–	–	–	9.36	0.45	1.16	–	–
	1–5 January 2010	347.5	2.3	389.3	0.2	−41.8	2.3	19.1	0.3	34.46	0.12	8.42	0.30	1.19	−9.0	0.5
	1–6 February 2010	–	–	–	–	–	–	–	–	–	–	9.06	0.14	1.16	–	–
	1–11 December 2010	331.2	4.0	388.7	0.5	−57.5	4.1	22.6	0.5	34.46	0.04	8.96	0.17	1.22	−14.6	1.3
	Seasonal average	340.7	4.8	388.0	0.6	−47.3	4.8	19.9	0.8	34.35	0.25	8.89	0.33	1.17	−10.6	1.3
Spring	15–27 March 2009	305.8	13.5	387.6	0.7	−81.8	13.5	21.3	1.0	34.36	0.10	9.15	0.20	1.13	−18.7	3.1
	20–30 April 2008	–	–	–	–	–	–	–	–	–	–	7.07	0.21	1.17	–	–
	21–30 April 2009	326.3	16.0	391.6	0.8	−65.4	16.1	21.5	1.3	33.99	0.52	7.57	0.37	1.15	−10.6	0.7
	6–10 April 2009	–	–	–	–	–	–	–	–	–	–	7.57	0.37	1.15	–	–
	12–15 April 2011	317.3	17.5	396.3	1.0	−79.0	17.6	18.4	1.5	34.43	0.34	6.88	0.08	1.18	−11.3	0.9
	1–20 May 2009	300.1	20.1	388.6	0.8	−88.6	20.1	21.0	1.3	33.81	0.44	5.98	0.22	1.16	−9.2	2.8
	26–31 May 2011	342.8	7.3	394.0	0.1	−51.3	7.3	22.7	0.4	34.24	0.18	6.17	0.35	1.21	−6.1	0.6
	Seasonal average	318.4	17.3	391.6	0.8	−73.2	17.4	21.0	1.3	34.17	0.39	7.20	0.30	1.16	−11.2	2.2
Summer	1–12 July 2009	388.7	5.0	366.7	0.2	22.0	5.0	27.1	0.3	33.95	0.14	6.75	0.12	1.14	2.8	0.6
	2–6 July 2007	375.0	12.5	372.9	0.2	2.1	12.5	28.2	0.3	33.76	0.12	6.95	0.25	1.27	0.4	2.1
	6–29 August 2008	392.7	2.4	374.7	0.2	18.1	2.4	28.7	0.2	33.48	0.17	5.51	0.16	1.18	1.6	0.2
	17–31 August 2009	400.4	5.8	361.0	0.3	39.4	5.8	29.5	0.3	33.66	0.13	6.05	0.23	1.47	6.7	2.1
	1–19 June 2011	345.1	9.8	386.6	1.2	−41.5	9.9	22.9	0.7	34.18	0.25	7.33	0.24	1.17	−6.5	0.2
	Seasonal average	380.4	8.9	372.4	0.6	8.0	8.9	27.3	0.4	33.81	0.19	6.52	0.23	1.25	1.0	1.5
Autumn	18–25 September 2006	–	–	–	–	–	–	–	–	–	–	6.39	0.42	1.26	–	–
	14–18 October 2006	327.6	35.5	381.8	0.2	−54.2	35.5	25.7	0.3	34.18	0.33	7.56	0.28	1.10	−7.9	0.1
	20–24 November 2006	–	–	–	–	–	–	–	–	–	–	7.06	0.14	1.18	–	–
	1–10 November 2007	–	–	–	–	–	–	–	–	–	–	10.37	0.53	1.08	–	–
	26–30 November 2010	336.4	2.4	386.8	0.3	−50.4	2.4	21.8	0.2	34.42	0.04	8.39	0.40	1.11	−9.3	0.5
	Seasonal average	336.4	2.4	386.8	0.3	−50.4	2.4	21.8	0.2	34.42	0.04	8.05	0.40	1.15	−9.3	0.5
Annual average		344.0	11.7	384.7	0.7	−40.7	11.7	22.5	0.9	34.18	0.29	7.66	0.37	1.18	−7.5	1.7

The annual mean CO_2 fluxes were -6.2 ± 9.1 in Domain I, -5.3 ± 3.7 in Domain II, -9.2 ± 4.2 in Domain III, -7.5 ± 1.7 in Domain IV and -5.9 ± 3.4 mmol m^{-2} d^{-1} in Domain V (Fig. 7). The area-weighted annual mean CO_2 flux was -6.9 ± 4.0 mmol m^{-2} d^{-1} (Fig. 7), which was more than twice the global average of ocean margins (Chen et al., 2013; Dai et al., 2013). Based on these CO_2 fluxes, the five domains absorbed 4.9 (± 4.4), 0.9 (± 0.4), 3.8 (± 1.0), 2.1 (± 0.3) and 1.5 (± 0.5) $\times 10^{12}$ g C yr^{-1} of atmospheric CO_2, and the ECS shelf absorbed 13.2 (± 4.6) $\times 10^{12}$ g C yr^{-1} of atmospheric CO_2.

5 Discussion

5.1 Major controls of surface water pCO_2

Because of the significant zonal difference in seasonality shown in both pCO_2 and CO_2 fluxes, we discuss the major controls of pCO_2 in the five domains categorized. This discussion is primarily based on the relationships of the in situ and normalized pCO_2 (NpCO_2, normalized to 21 °C in this study) with the other parameters in each domain. Since the Changjiang plume and coastal regions are strongly influenced by biological activities and/or the terrestrial high-pCO_2 waters (Tseng et al., 2014; Zhai and Dai, 2009), we used the data collected from the offshore area (Domains IV and V) to obtain the "background" NpCO_2. In these two domains, NpCO_2 ranged from 250 to 400 µatm, and so we used $250 \times \exp((\text{SST-}21) \times 0.0423)$ and $400 \times \exp((\text{SST-}21) \times 0.0423)$ µatm as the lower and upper limits of thermodynamically dominated pCO_2 on the entire ECS shelf.

In Domains I and II, pCO_2 showed no conspicuous trend with SST on the yearly timescale (Fig. 8). However, within individual seasons, the temperature effect on pCO_2 can be revealed. In winter, most data were above the upper limit of the thermodynamically dominated pCO_2, suggesting extra CO_2 added to the surface water. In summer, many data were below the lower limit of the thermodynamically dominated pCO_2, indicating biogeochemical uptake of CO_2. The pCO_2 in these two domains neither showed clear trends with salin-

Table 7. Data summary of Domain V. "Atm. pCO$_2$" is atmospheric pCO$_2$; SST is sea surface temperature; SSS is sea surface salinity; F_{CO_2} is the air–sea CO$_2$ flux; and SD is standard deviation. C$_2$ is the nonlinearity effect of the short-term variability in wind speeds over 1 month on the gas transfer velocity, assuming that long-term winds followed a Raleigh (Weibull) distribution (Wanninkhof, 1992; Jiang et al., 2008). See text for details. October 2006 and December 2010 were excluded in the calculations of seasonal averages. pCO$_2$ data are corrected to the reference year 2010.

Season	Period	pCO$_2$ (µatm)		Atm pCO$_2$ (µatm)		ΔpCO$_2$ (µatm)		SST (°C)		SSS		Wind speed (m s^{-1})		C$_2$	FCO$_2$ (mmol m^{-2} d^{-1})	
		Mean	SD	Mean	SD	Mean	SD	Mean	SD	Mean	SD	Mean	SD	Mean	Mean	SD
Winter	23–31 December 2008	340.5	4.3	386.5	0.5	−46.0	4.36	21.2	0.9	34.00	0.17	9.21	0.52	1.14	−10.9	1.0
	4–31 December 2009	340.8	2.9	387.3	0.3	−46.5	2.92	23.1	0.3	34.66	0.06	8.74	0.44	1.16	−10.2	2.4
	1–3 January 2006	–	–	–	–	–	–	–	–	–	–	9.30	0.46	1.11	–	–
	1–14 January 2009	–	–	–	–	–	–	–	–	–	–	10.02	0.49	1.09	–	–
	1–5 January 2010	349.6	11.2	389.3	0.2	−39.7	11.21	21.0	1.1	34.58	0.04	8.78	0.50	1.17	−9.0	2.5
	1–6 February 2010	–	–	–	–	–	–	–	–	–	–	8.39	0.80	1.20	–	–
	1–11 December 2010	–	–	–	–	–	–	–	–	–	–	8.41	0.49	1.24	–	–
	Seasonal average	343.6	8.7	387.7	0.5	−44.1	8.75	21.7	1.0	34.41	0.13	9.07	0.60	1.16	−10.0	2.5
Spring	15–27 March 2009	326.5	20.6	386.7	1.0	−60.3	20.61	24.2	1.8	34.21	0.09	8.82	0.56	1.12	−12.5	4.3
	20–30 April 2008	–	–	–	–	–	–	–	–	–	–	6.96	0.47	1.17	–	–
	21–30 April 2009	354.9	6.4	387.8	1.6	−32.9	6.59	24.9	2.2	34.32	0.06	8.03	0.32	1.12	−5.6	1.1
	6–10 April 2009	–	–	–	–	–	–	–	–	–	–	8.03	0.32	1.12	–	–
	12–15 April 2011	339.8	7.0	392.5	1.0	−52.7	7.08	24.1	0.8	34.70	0.06	6.88	0.33	1.17	−7.2	−7.2
	1–20 May 2009	342.8	7.6	385.3	0.9	−42.5	7.70	24.0	1.2	34.27	0.08	6.09	0.27	1.14	−4.4	0.9
	26–31 May 2011	362.0	6.0	394.0	0.1	−32.1	6.04	24.6	0.7	34.22	0.11	6.46	0.33	1.21	−4.2	0.4
	Seasonal average	345.2	12.3	389.3	1.2	−44.1	12.39	24.4	1.6	34.34	0.09	7.32	0.41	1.15	−6.8	4.3
Summer	1–12 July 2009	380.5	12.9	366.5	0.5	14.0	12.96	27.6	1.0	34.00	0.20	6.52	0.43	1.23	1.9	0.2
	2–6 July 2007	388.5	11.6	373.9	1.6	14.7	11.67	28.4	1.8	34.18	0.28	6.14	0.64	1.26	1.9	0.2
	6–29 August 2008	374.3	10.2	374.4	0.4	−0.1	10.23	28.6	0.4	33.05	0.33	5.33	0.31	1.24	−0.0	0.2
	17–31 August 2009	378.8	19.8	363.7	0.7	15.0	19.80	28.1	0.7	33.53	0.22	5.91	0.43	1.70	3.2	4.8
	1–19 June 2011	–	–	–	–	–	–	–	–	–	–	6.90	0.55	1.19	–	–
	Seasonal average	380.5	16.3	369.6	1.1	10.9	16.34	28.2	1.3	33.69	0.30	6.16	0.54	1.32	1.8	2.8
Autumn	18–25 September 2006	–	–	–	–	–	–	–	–	–	–	6.93	0.60	1.19	–	–
	14–18 October 2006	–	–	–	–	–	–	–	–	–	–	7.80	0.52	1.09	–	–
	20–24 November 2006	–	–	–	–	–	–	–	–	–	–	7.27	0.38	1.16	–	–
	1–10 November 2007	–	–	–	–	–	–	–	–	–	–	11.42	0.66	1.06	–	–
	26–30 November 2010	347.9	6.1	385.9	0.6	−38.1	6.16	24.6	0.8	34.43	0.07	9.46	0.75	1.08	−8.4	2.0
	Seasonal average	347.9	6.1	385.9	0.6	−38.1	6.16	24.6	0.8	34.43	0.07	8.77	0.75	1.12	−8.4	2.0
Annual average		354.3	13.3	383.1	1.0	−28.8	13.35	24.7	1.4	34.22	0.20	7.83	0.68	1.19	−5.9	3.4

ity, but in winter, it generally decreased with SSS (Fig. 9). It is thus suggested that other processes in addition to SST and estuarine mixing also played important roles in the pCO$_2$ variability, including aerobic respiration, biological productivity, terrestrial input and ventilation, amongst other factors.

The Changjiang river and estuarine water were characterized by high pCO$_2$ resulting mainly from aerobic respiration (Zhai et al., 2007). In Domain I, the area off the Changjiang estuary and the coastal area were influenced by the high-pCO$_2$ estuarine water (Fig. 2). On the other hand, in warm seasons, the plume water was stratified and biological productivity lowered the surface water pCO$_2$ as indicated by the high Chl a concentration in spring and summer (Fig. 10). NpCO$_2$ generally decreased with the increase in Chl a concentration. Although pCO$_2$ showed no relationship with SST or SSS, NpCO$_2$ showed a decreasing pattern with SST and the lowest NpCO$_2$ occurred in the warm seasons, which was consistent with the highest productivity (Figs. 8 and 10). In autumn, vertical stratification collapsed and the CO$_2$-enriched subsurface and bottom waters mixed into the

surface and increased the surface water pCO$_2$. In winter and early autumn, the cooling effect decreased pCO$_2$ and resulted in Domain I acting as a CO$_2$ sink in the cold seasons. If the pCO$_2$ in winter was taken as the reference, the calculated thermodynamically controlled pCO$_2$ in spring would be 379.3 µatm. The observed pCO$_2$ in spring was 70.4 µatm lower than the thermodynamically mediated pCO$_2$. Similarly, if spring was taken as a reference, the thermodynamically mediated pCO$_2$ in summer would be 479.0 µatm, and the observed pCO$_2$ was 161.8 µatm lower than this value. These differences might be due to the CO$_2$ drawdown mainly mediated by biological activities. Similarly, the observed pCO$_2$ was 100.5 µatm higher than the thermodynamically mediated pCO$_2$ (293.0 µatm) in autumn, which might be due mainly to the mixing of the CO$_2$-rich subsurface and/or bottom water in autumn, when vertical mixing was enhanced. It should be noted that the CO$_2$ system is a buffer system and the pCO$_2$ response is much slower (Zhai et al., 2014). Therefore, the above estimation is to explain the biological
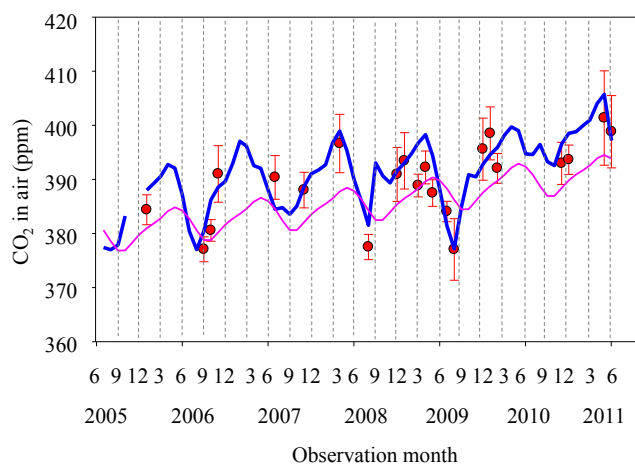
Figure 5. Temporal distribution of atmospheric CO_2 concentrations based on shipboard measurements during the cruise to the East China Sea (arithmetic average, red solid dots) and its comparison with the measurements at 21 m above sea level, at Tae-ahn Peninsula (blue solid line; 36.7376° N, 126.1328° E; Republic of Korea, http://www.esrl.noaa.gov/gmd/dv/site) and at Mauna Loa Observatory at Hawaii (pink solid line; Scripps CO_2 program, http://scrippsco2.ucsd.edu). The error bars are the standard deviations. The CO_2 concentrations in this plot are the original values in the year of the observations.

effect on pCO_2 qualitatively rather than to make an accurate calculation.

Controls of pCO_2 in Domain II were similar to but more complex than those in Domain I. Cooling and biological uptake were responsible for the strong sink in winter and spring. However, in summer biological uptake of CO_2 was limited since it was beyond the productive area (Fig. 10), so the CO_2 flux was controlled by both biological activities and heating effect. In autumn, cooling was important in drawing down pCO_2 and the influence of vertical mixing was not significant since the hypoxia and thus the high-pCO_2 bottom water was limited to Domain I (Chen et al., 2007; Wang et al., 2012).

In Domains IV and V, pCO_2 in summer was higher than that in the other seasons (Fig. 2). The pCO_2 generally increased with SST but showed no trend with SSS (Figs. 8 and 9). This suggests that temperature was an important factor influencing pCO_2. Neither pCO_2 nor NpCO_2 showed conspicuous trends with Chl a concentration, and Chl a concentration was relatively low ($< 2 \mu g$ L^{-1}, Fig. 10). This suggests that, for a particular season, productivity was not the dominating process in the spatial distribution of pCO_2. Comparison among the seasons showed that the NpCO_2 was highest in winter and lowest in summer. This might be due to the weak mixing of the CO_2-rich subsurface water in summer. Additionally, the lowest NpCO_2 values in summer might suggest that the potential biological uptake of CO_2 was strong in summer, although biological uptake was not a
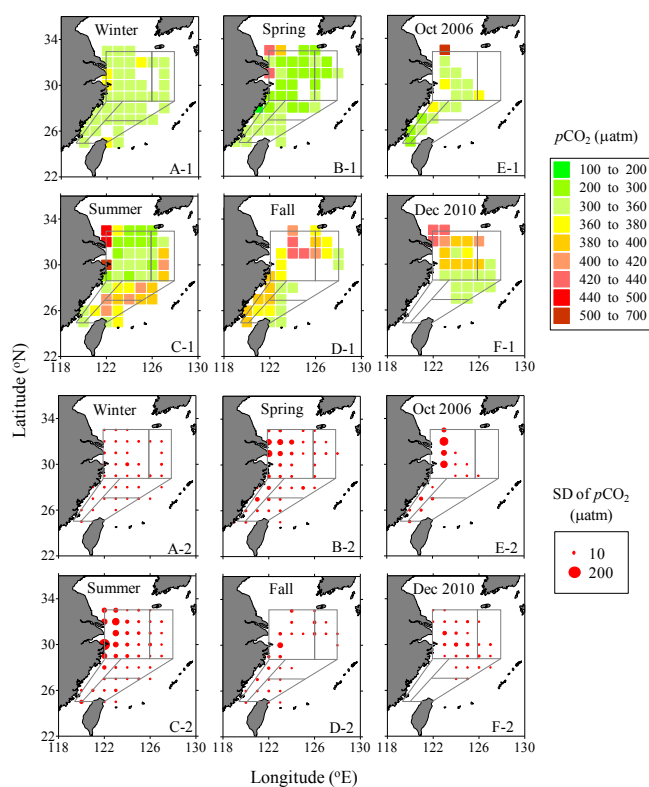
Figure 6. Distribution of seasonal average and standard deviations (SD) of pCO_2 in 1° × 1° grids on the East China Sea shelf. The framed areas show the five physical–biogeochemical domains. Panel **(a-1)** and **(a-2)** are the result of the winter cruises, excluding December 2010; panels **(d-1)** and **(d-2)** are results of the autumn cruises, excluding October 2006. Data are corrected to the reference year 2010. The surveys conducted in October 2006 and November 2010 were excluded in the seasonal average calculations and were presented separately, which was due mainly to the abnormal character of these two surveys. See details in the text.

dominating factor. Although NpCO_2 was lowest in summer, in situ pCO_2 was highest, indicating that high temperature increased pCO_2 in the warm seasons. With similar calculations conducted in Domain I, the estimated pCO_2 drawdown would be 25 to 39 µatm in spring and summer and the pCO_2 increase in autumn would range from 21 to 35 µatm due to enhanced vertical mixing. These values were much lower than the dynamic inshore areas (Domains I and II) and might be negligible; the re-equilibrium of CO_2 takes a longer time than the 3-month-long seasons defined here (Zhai et al., 2014). The major controls of pCO_2 in Domain III were between those of Domains I/II and IV/V.

In summary, the ECS shelf is heterogeneous in both CO_2 fluxes and their controls. The pCO_2 of the inner shelf waters (Domains I and II) was mainly dominated by the biological uptake of CO_2 in spring and/or summer and cooling in winter, which induced the moderate to strong sink in the three seasons, while in autumn mixing with CO_2-rich bottom
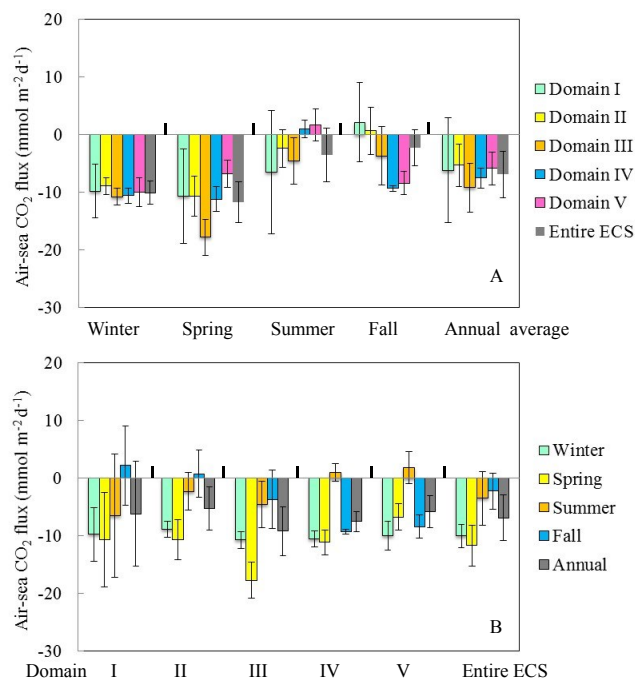
Figure 7. CO$_2$ fluxes and seasonal variations in the East China Sea. The error bars are the standard deviations.

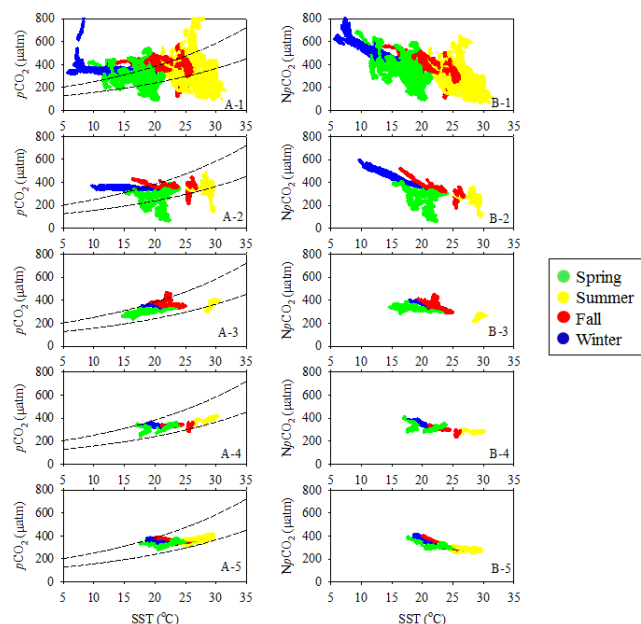**Figure 8.** Relationships of pCO$_2$ and NpCO$_2$ (pCO$_2$ normalized to 21 °C) of the surface water with sea surface temperature (SST). Panels **(a-1)** and **(b-1)** are Domain I; panels **(a-2)** and **(b-2)** are Domain II; panels **(a-3)** and **(b-3)** are Domain III; panels **(a-4)** and **(b-4)** are Domain IV; panels **(a-5)** and **(b-5)** are Domain V. The dashed lines in panels **(a-1)** to **(a-5)** represent $250 \times \exp((\text{SST-21}) \times 0.0423)$ and $400 \times \exp((\text{SST-21}) \times 0.0423)$ µatm, in which 250 and 400 µatm are the lower and higher limits of NpCO$_2$ in Domains IV and V (see details in the text). pCO$_2$ and NpCO$_2$ values are those of the year of observations.

and/or subsurface water was attributed to the CO$_2$ release. However, the offshore areas (Domains IV and V) were dominated mainly by temperature.

The CO$_2$ sink is dominated by the high biological productivity in summer (Chou et al., 2009), which appears to have close correlation with the Changjiang riverine discharge (Tseng et al., 2011; Tseng et al., 2014). However, cooling is attributed to be the major driver of the CO$_2$ sink in winter (Tsunogai et al., 1999). In the northern ECS and in the area off the Changjiang estuary, vertical mixing of the CO$_2$-rich subsurface and/or bottom waters is attributed to the CO$_2$ source in autumn (Kim et al., 2013; Zhai and Dai, 2009). Shim et al. (2007) suggest that pCO$_2$ in the northeastern ECS is dominated by temperature but in the northwestern ECS, the main controlling factor is more seasonally complex. Based on the data collected from single cruise in summer, autumn and winter, Chou et al. (2013) suggest that pCO$_2$ is dominated by biological production on the inner shelf and by temperature on the outer shelf.

Based on the data collected mainly on the inner and middle ECS shelves and limited field surveys in cold seasons, Tseng et al. (2014) suggest that the Changjiang discharge is the primary factor that governs the CO$_2$ sink for the entire ECS. The data set covering complete seasonal and spatial coverage presented in this study suggested that zonal assessment is important to obtain a comprehensive picture of CO$_2$ flux and its control in the dynamic marginal seas. Extrapolation from the data collected in the river-dominated area to the entire ECS shelf could be misleading.

5.2 Intra-seasonal variation in CO$_2$ fluxes

With the five domains categorized, we have seen overall well-defined seasonality in both pCO$_2$ and CO$_2$ fluxes in the individual domains, and significant intra-seasonal changes occurred, which could affect the overall carbon budgeting on a longer seasonal and/or annual timescale.

The intra-seasonal variation in the CO$_2$ fluxes was generally low in winter (typically < 2-fold variations), but it was very high in summer (4- to 6-fold) and spring (2- to 3-fold). Spatially, the largest intra-seasonal variability was in Domain I. The intra-seasonal variation in the calculated CO$_2$ flux in this study was attributed to the intra-seasonal variability in ΔpCO$_2$, wind speeds, and C$_2$. In the five domains, the highest value of C$_2$ was 1.1- to 1.4-fold the lowest value within each season, which did not induce remarkable intra-seasonal variability in the calculated CO$_2$ flux. However, intra-seasonal variability in wind speed and ΔpCO$_2$ might have induced large variability in the calculated CO$_2$ fluxes. The highest wind speed was 1.1- to 1.2-fold the lowest value in winter and 1.2- to 1.6-fold those in spring, summer and autumn in each domain. This might have caused 1.2- to 1.4-fold variation in winter and 1.4- to 2.6-fold variation in other
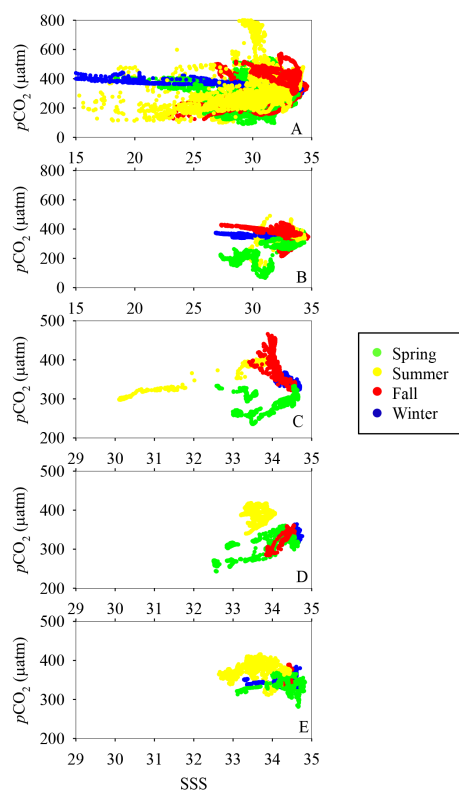
Figure 9. Relationships of pCO_2 of the surface water with sea surface salinity (SSS). Panels **(a)**, **(b)**, **(c)**, **(d)** and **(e)** are Domains I to V, respectively. pCO_2 values are those of the year of observations.

Figure 10. Relationships of pCO_2 and $NpCO_2$ (pCO_2 normalized to 21 °C) with chlorophyll a (Chl a) concentration. The data of Chl a concentration in surface water were unpublished data from Dr. Jun Sun. The spring surveys include April and May 2011; the summer surveys include July and August 2009; the autumn surveys include November 2010; and the winter surveys include December 2009 and January 2010. Panels **(a-1)** and **(b-1)** are Domain I; panels **(a-2)** and **(b-2)** are Domain II; panels **(a-3)** and **(b-3)** are Domain III; panels **(a-4)** and **(b-4)** are Domain IV; panels **(a-5)** and **(b-5)** are Domain V. pCO_2 and $NpCO_2$ values are those of the year of observations.

seasons in the calculated CO_2 fluxes. The intra-seasonal variability in wind speed showed no spatial pattern. The intra-seasonal variation in ΔpCO_2 was generally high in summer and spring but low in winter and autumn. The largest intra-seasonal variation was observed in Domain I in summer and spring. In summer, the lowest ΔpCO_2 was −85 µatm in June 2006, which was 6.9-fold that in July 2009 (−12 µatm). The intra-seasonal variation in ΔpCO_2 in spring was smaller than in summer but still very large (3.5-fold).

Additionally, atypical surveys increased the intra-seasonal variations. One example was the October 2006 cruise. Under typical autumn conditions, Domain I is a source of atmospheric CO_2 when stratification starts to weaken and strong vertical mixing starts leading to the release of subsurface CO_2 (Zhai and Dai, 2009). In October 2006, however, average pCO_2 was down to 364 µatm in Domain I, which was 29 µatm lower than the seasonal average based on the data collected during all the other surveys in autumn (394 µatm; Table 3). The low pCO_2 in October 2006 might be induced by a local bloom as reflected by the high degree of oxygen saturation in the surface water. Dissolved oxygen increased to 120 %–130 % in a local area off Hangzhou Bay and the Changjiang estuary, which was a significant increase from September 2006 when the de-
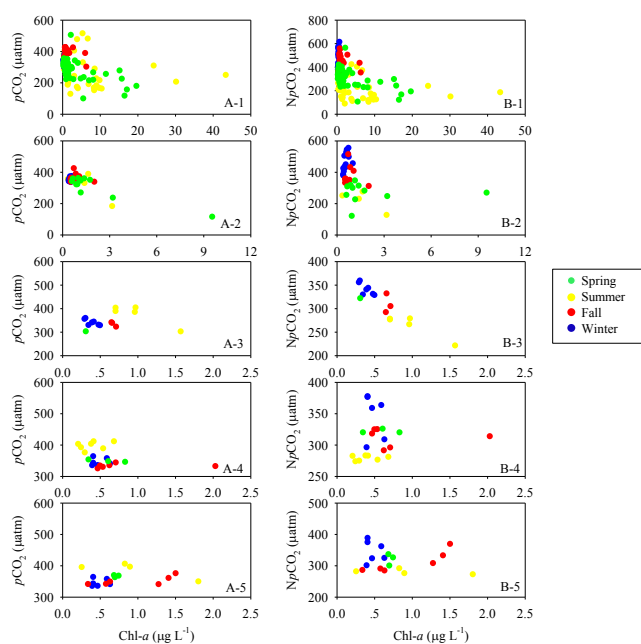
gree of oxygen saturation ranged from 90 to 110 % (Fig. A1 in the Appendix). This local bloom caused Domain I to act as a CO_2 sink of 1.9 mmol m^{-2} d^{-1} as compared to a CO_2 source of 2.2 mmol m^{-2} d^{-1} based on the data collected from all the other autumn surveys (Table 3). If this survey was included into the flux estimation, the seasonal average CO_2 flux in autumn would be 1.2 ± 6.4 in Domain I. This CO_2 source strength was ∼ 54 % of the average of the other autumn cruises in Domain I. However, the inclusion of the October 2006 survey into the autumn cruises would result in an annual CO_2 flux of -7.1 ± 3.9 mmol m^{-2} d^{-1}, which is not significantly different from the estimate of -6.9 ± 4.0 mmol m^{-2} d^{-1} excluding the October 2006 cruise. This was because we had multiple cruise observations in autumn and the autumn bloom was only observed in a very small area of the ECS.

In the temperate seas, blooms occur in both spring and autumn, which are mainly controlled by light availability and nutrient supply (Lalli and Parsons, 1993; Martinez et al., 2011). In the ECS, there is no report on autumn blooms in the near-shore area. The occurrence of a autumn bloom and its influence on the CO_2 flux needs further study.

Table 8. Comparison of air–sea CO$_2$ fluxes on the East China Sea shelf. Methods: 1: pCO$_2$ measurements and gas transfer algorithms with wind speeds; 2: pCO$_2$ calculated from dissolved inorganic carbon, total alkalinity, and gas transfer algorithms with wind speeds; 3: pCO$_2$ algorithms (with Changjiang discharge and SST) and gas transfer algorithms with wind speeds; 4: pCO$_2$ measurements and algorithms (with SST, SSS and phosphate) and given gas transfer velocity.

Study area	Season	Methods	Wind speed	k[a]	FCO$_2$ (mmol m^{-2} d^{-1})	FCO$_2$_S(07)[b] (mmol m^{-2} d^{-1})	Data source
	Spring	1	Short-term	W92_S	-8.8 ± 5.8	-7.7 ± 5.1	Zhai and Dai (2009)
	Spring	1	Monthly	S07		-10.7 ± 8.2	This study
	Summer	1	Short-term	W92_S	-4.9 ± 4.0	-4.3 ± 3.5	Zhai and Dai (2009)
	Summer	1	Monthly	S07		-6.5 ± 10.7	This study
Domain I	Autumn	1	Short-term	W92_S	2.9 ± 2.5	2.5 ± 2.2	Zhai and Dai (2009)
	Autumn	1	Monthly	S07		2.2 ± 6.8	This study
	Winter	1	Short-term	W92_S	-10.4 ± 2.3	-9.1 ± 2.0	Zhai and Dai (2009)
	Winter	1	Monthly	S07		-9.8 ± 4.6	This study
	Annual	1	Short-term	W92_S	-5.2 ± 3.6	-4.5 ± 3.1	Zhai and Dai (2009)
	Annual	1	Monthly	S07		-6.2 ± 9.1	This study
	Spring	1	Monthly	W92_L	-5.0 ± 1.6	-4.2 ± 1.3	Shim et al. (2007)
	Spring	1	Daily	W92_S	-6.8 ± 4.3	-5.9 ± 3.7	Kim et al. (2013)
	Spring	1	Monthly	S07		-13.0 ± 6.6	This study
Domains I and III	Summer	1	Daily	W92_S	-6.6 ± 8.5	-5.7 ± 7.4	Kim et al. (2013)
	Summer	1	Monthly	S07		-5.8 ± 8.5	This study
	Autumn	1	Monthly	W92_L	1.1 ± 2.9	0.9 ± 2.4	Shim et al. (2007)
	Autumn	1	Daily	W92_S	0.8 ± 7.3	0.7 ± 6.4	Kim et al. (2013)
	Autumn	1	Monthly	S07		0.2 ± 6.2	This study
	Winter	1	Daily	W92_S	-12 ± 4.1	-10.5 ± 3.6	Kim et al. (2013)
	Winter	1	Monthly	S07		-10.1 ± 3.6	This study
	Annual	4	–	–	-8	–	Tsunogai et al. (1999)
	Annual	1	Daily	W92_S	-6.0 ± 5.8	-5.2 ± 5.0	Kim et al. (2013)
	Annual	1	Monthly	S07		-7.2 ± 6.2	This study
Domains I, III and IV	Summer	2	–	L&M86; T90	-1.8 to -4.8	–	Wang et al. (2000)
	Summer	1	Monthly	S07		-4.6 ± 5.9	This study
Domains II, IV and V	Spring	2	Long-term	–	-5.8 ± 7.7	–	Peng et al. (1999)
	Spring	1	Monthly	S07		-9.5 ± 2.0	This study
	Spring	3	Monthly	S07	–	-8.2 ± 2.1	Tseng et al. (2014)
	Spring	3	Long-term	W92_L	-11.5 ± 2.5	-9.6 ± 2.1	Tseng et al. (2011)
	Spring	1	Monthly	S07		-11.7 ± 3.6	This study
	Summer	1	Daily	S07		-2.4 ± 3.1	Chou et al. (2009)
	Summer	3	Long-term	W92_L	-1.9 ± 1.4	-1.6 ± 1.2	Tseng et al. (2011)
	Summer	3	Monthly	S07		-2.5 ± 3.0	Tseng et al. (2014)
	Summer	1	Monthly	S07		-3.5 ± 4.6	This study
ECS shelf	Autumn	3	Long-term	W92_L	-2.2 ± 3.0	-1.8 ± 2.5	Tseng et al. (2011)
	Autumn		Monthly	S07		-0.8 ± 1.9	Tseng et al. (2014)
	Autumn	1	Monthly	S07		-2.3 ± 3.1	This study
	Winter	1	Monthly	W92_L	-13.7 ± 5.7	-11.4 ± 4.7	Chou et al. (2011)
	Winter	3	Long-term	W92_L	-9.3 ± 1.9	-7.7 ± 1.6	Tseng et al. (2011)
	Winter	3	Monthly	S07		-5.5 ± 1.6	Tseng et al. (2014)
	Winter	1	Monthly	S07		-10.0 ± 2.0	This study
	Annual	3	Long-term	W92_L	-6.3 ± 1.1	-5.2 ± 0.9	Tseng et al. (2011)
	Annual	3	Monthly	S07		-3.8 ± 1.1	Tseng et al. (2014)
	Annual	1	Monthly	S07		-6.9 ± 4.0	This study

[a] W92_S is the Wanninkhof (1992) algorithm for short-term wind speeds; W92_L is the Wanninkhof (1992) algorithm for long-term (or monthly average) wind speeds; S07 is the Sweeney et al. (2007) algorithm; L&M86 is the Liss and Merlivat (1986) algorithm; T90 is the Tans et al. (1990) algorithm. [b] FCO$_2$ data were calculated (or recalculated) with the Sweeney et al. (2007) gas transfer algorithm with wind speed.

Another example is the early winter cruise (based on our seasonal category) in 2010 which was conducted from 1 to 11 December. The average SST was 5.5 °C higher than the average SST during other winter surveys in Domain I. Also, the pCO$_2$ distribution pattern was similar to that in autumn. As a result, Domain I was a weak sink of -1.6 mmol m^{-2} d^{-1} during this early December cruise, which was only 16 % of the average CO$_2$ sink based on the data collected during the other winter cruises (-9.8 mmol m^{-2} d^{-1}). We concluded that this early December 2010 survey was conducted during the transitional period between typical autumn and winter, which would be difficult to categorize into any season. If the December 2010 survey was grouped into the autumn cruises, the seasonal average CO$_2$ flux in Domain I in autumn would be 1.2 ± 7.1 mmol m^{-2} d^{-1} and the annual CO$_2$ flux in the entire ECS would be -7.4 ± 4.1 mmol m^{-2} d^{-1}. However, if the December 2010 survey was grouped into the winter cruises, the seasonal average CO$_2$ flux in Domain I in winter would be -8.4 ± 5.3 mmol m^{-2} d^{-1} and the annual CO$_2$ flux in the entire ECS would be -6.9 ± 4.1 mmol m^{-2} d^{-1}.

The strong CO$_2$ sink in the ECS might be attributed to the generally low surface water pCO$_2$. As discussed in Section 5.1, the strong biological uptake in spring and/or summer and strong cooling in winter were the major controls on the low pCO$_2$ in the ECS. Primary production on the ECS shelf ranges from 0.2 to 2.0 g C m^{-2} d^{-1} in warm seasons (Gong et al., 2003). During our spring and summer cruises, Chl a concentration was up to 20 or even 40 µg L^{-1}. Both the phytoplankton biomass and the primary production are among the highest in the world's marginal seas, e.g. the Barents Sea (Dalpadado et al., 2014) , the Beaufort Sea (Carmack et al., 2004), the South Atlantic Bight (Martins and Pelegri, 2006), and the South China Sea (Chen, 2005). In addition, the ECS is located in the midlatitude zone with strong seasonality. In winter, the low temperature draws surface water pCO$_2$ well below the atmospheric pCO$_2$, drawing down ~ 140 µatm with 10 °C decrease from ~ 400 µatm.

This study reports what we believe to be the most comprehensive data set of CO$_2$ fluxes based on field measurements with a full coverage of the ECS shelf at a temporal resolution of seasonal scale. Table 8 shows comparisons of the CO$_2$ fluxes estimated in this study with others in the ECS. For ease of comparison, we standardized the CO$_2$ flux estimation using the Sweeney et al. (2007) gas transfer velocity algorithms. For the results calculated using long-term (or monthly) average wind speeds, we multiplied C_2 (~ 1.2) to make them consistent with our estimation. The CO$_2$ fluxes calculated using the algorithm of Ho et al. (2006) were the same as those of Sweeney et al. (2007).

Comparison between our results and the CO$_2$ fluxes estimated based on multiple observations (such as those of Zhai and Dai 2009) were similar in Domain I in all seasons (the differences were < 35 %, Table 8). However, the CO$_2$ flux estimations based on limited surveys in spring – the season with strong intra-seasonal variability – such as those of Kim

et al. (2013) and Shim et al. (2007) in Domains I and III and Peng et al. (1999) in Domains III, IV and V, were often different from our results. However, the CO$_2$ fluxes based on a single survey in winter by Chou et al. (2011) on the entire ECS shelf and on that by Kim et al. (2013) in Domains I and III were similar to our results, which is likely due to the relatively smaller inter-seasonal variability in winter. For the entire ECS, the CO$_2$ fluxes in spring and summer estimated by Tseng et al. (2011, 2014) are similar to our estimate based on field surveys. However, there is a large difference in the autumn results. The good consistency of the Tseng et al. (2011; 2014) results with ours in spring and summer might be due to the fact that their empirical algorithm is mainly based on field data collected in warmer seasons.

We have demonstrated that field observations with a full consideration of seasonal variability are necessary to constrain CO$_2$ fluxes with large heterogeneity in both time and space. We must point out, however, that it remains difficult to fully resolve the intra-seasonal changes in dynamic shelf seas, in particular in areas such as Domains I and II. High-frequency observation in the seasons and/or locations with largest variability or those for which we have a poor understanding of the mechanisms controlling pCO$_2$ are clearly needed to reduce the error from undersampling and to further improve estimates of CO$_2$ fluxes.

6 Concluding remarks

Surface water pCO$_2$ and air–sea CO$_2$ fluxes on the ECS shelf show strong temporal and spatial variations, despite which the pCO$_2$ and associated fluxes are robustly well defined. The Changjiang plume is a moderate to strong CO$_2$ sink in spring, summer and winter, but it is a weak CO$_2$ source in autumn. The middle and southern ECS shelves are a CO$_2$ source in summer but a strong CO$_2$ sink in other seasons. Major controls of pCO$_2$ differ in different domains. Domains I and II were mainly dominated by biological CO$_2$ uptake in spring and summer, ventilation in autumn and cooling in winter, while Domains IV and V were dominated by temperature over the whole year. On an annual basis, the entire ECS shelf is a CO$_2$ sink of 6.9 (± 4.0) mmol m^{-2} d^{-1} and it sequesters 13.2 Tg C from the atmosphere annually based on our observations from 2006 to 2011. This study suggested that zonal assessment of CO$_2$ fluxes and a study of the major controls were necessary in the dynamic marginal seas.

Appendix A: Spatial distribution of sea surface dissolved oxygen saturation during our cruises in September and October 2006

To verify an algal bloom associated with our October 2006 cruise, we presented the dissolved oxygen data from our cruises in September and October 2006 (Fig. A1). The high degree of oxygen saturation (DO%) was observed in the surface water in the area off the Hangzhou Bay and the Changjiang estuary. Dissolved oxygen increased from air equilibrium (DO% from 90 to 110 %) in September 2006 to oversaturation (DO% from 120 to 130 %) in October 2006, indicating that an algal bloom occured there.
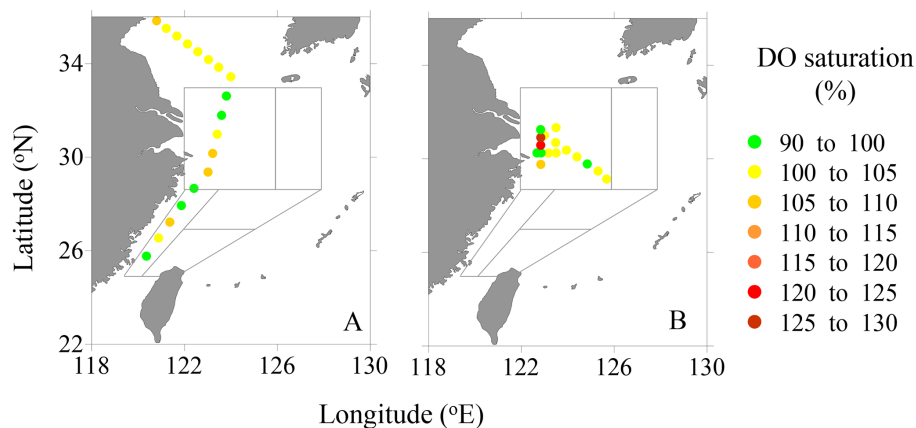
Figure A1. Spatial distribution of degree of oxygen saturation in the surface water during the cruises in September (**a**) and October 2006 (**b**). The framed areas show the five physical–biogeochemical domains. The dissolved oxygen (DO) saturation was calculated from the measured DO concentration (via Winkler titration method on board) and the oxygen solubility via the Bensen and Krause (1984) equation.

References

Bai, Y., He, X., Pan, D., Chen, C.-T. A., Kang, Y., Chen, X., and Cai, W.-J.: Summertime Changjiang River plume variation during 1998–2010, J. Geophys. Res. Oceans, 119, 6238–6257, 2014.

Benson, B. B. and Krause, D.: The concentration and isotopic fractionation of oxygen dissolved in fresh water and seawater in equilibrium with the atmosphere, Limnol. Oceanogr., 29, 620–632, 1984.

Borges, A. V., Delille, B., and Frankignoulle, M.: Budgeting sinks and sources of CO$_2$ in the coastal ocean: Diversity of ecosystems counts, Geophys. Res. Lett., 32, L14601, doi:10.1029/2005GL023053, 2005.

Cai, W.-J. and Dai, M.: Comment on "Enhanced open ocean storage of CO$_2$ from shelf sea pumping", Science, 306, 1477–1477, 2004.

Cai, W.-J., Dai, M.-H., and Wang, Y.-C.: Air-sea exchange of carbon dioxide in ocean margins: A province-based synthesis, Geophys. Res. Lett., 33, L12603, doi:10.1029/2006GL026219, 2006.

Carmack, E. C., Macdonald, R. W., and Jasper, S.: Phytoplankton productivity on the Canadian Shelf of the Beaufort Sea, Mar. Ecol.-Prog. Ser., 277, 37–50, 2004.

Chen, C.-C., Gong, G.-C., and Shiah, F.-K.: Hypoxia in the East China Sea: One of the largest coastal low-oxygen areas in the world, Mar. Environ. Res., 64, 399–408, 2007.

Chen, C.-T. A. and Borges, A. V.: Reconciling opposing views on carbon cycling in the coastal ocean: Continental shelves as sinks and near-shore ecosystems as sources of atmospheric CO$_2$, Deep-Sea Res. Pt. II, 56, 578–590, 2009.

Chen, C.-T. A. and Wang, S.-L.: Carbon, alkalinity and nutrient budgets on the East China Sea continental shelf, J. Geophys. Res., 104, 20675–20686, 1999.

Chen, C.-T. A., Zhai, W.-D., and Dai, M.-H.: Riverine input and air-sea CO$_2$ exchanges near the Changjiang (Yangtze River) Estuary: Status quo and implication on possible future changes in metabolic status, Cont. Shelf Res., 28, 1476–1482, 2008.

Chen, C.-T. A., Huang, T.-H., Chen, Y.-C., Bai, Y., He, X., and Kang, Y.: Air-sea exchanges of CO$_2$ in the world's coastal seas, Biogeosciences, 10, 6509–6544, doi:10.5194/bg-10-6509-2013, 2013.

Chen, Y.-L. L.: Spatial and seasonal variations of nitrate-based new production and primary production in the South China Sea, Deep-Sea Res. Pt. I, 52, 319–340, 2005.

Chou, W. C., Sheu, D. D., Lee, B. S., Tseng, C. M., Chen, C. T. A., Wang, S. L., and Wong, G. T. F.: Depth distributions of alkalinity, TCO$_2$ and δ^{13}C$_{TCO_2}$ at SEATS time-series site in the northern South China Sea, Deep-Sea Res. Pt. II, 54, 1469–1485, 2007.

Chou, W.-C., Gong, G.-C., Sheu, D. D., Hung, C.-C., and Tseng, T.-F.: Surface distributions of carbon chemistry parameters in the East China Sea in summer 2007, J. Geophys. Res., 114, C07026, doi:10.1029/2008JC005128, 2009.

Chou, W.-C., Gong, G.-C., Tseng, C.-M., Sheu, D.-D., Hung, C.-C., Chang, L.-P., and Wang, L.-W.: The carbonate system in the East China Sea in winter, Mar. Chem., 123, 44–55, 2011.

Chou, W.-C., Gong, G.-C., Cai, W.-J., and Tseng, C.-M.: Seasonality of CO$_2$ in coastal oceans altered by increasing anthropogenic nutrient delivery from large rivers: evidence from the Changjiang-East China Sea system, Biogeosciences, 10, 3889–3899, doi:10.5194/bg-10-3889-2013, 2013.

Dai, A. and Trenberth, K. E.: Estimates of freshwater discharge from continents: Latitudinal and seasonal variations, J. Hydrometeorol., 3, 660–687, 2002.

Dai, M., Cao, Z., Guo, X., Zhai, W., Liu, Z., Yin, Z., Xu, Y., Gan, J., Hu, J., and Du, C.: Why are some marginal seas sources of atmospheric CO$_2$?, Geophys. Res. Lett., 40, 2154–2158, 2013.

Dai, M.-H., Lu, Z.-M., Zhai, W.-D., Chen, B.-S., Cao, Z.-M., Zhou, K.-B., Cai, W.-J., and Chen, C.-T. A.: Diurnal variations of surface seawater pCO$_2$ in contrasting coastal environments, Limnol. Oceanogr., 54, 735–745, 2009.

Dalpadado, P., Arrigo, K. R., Hjollo, S. S., Rey, F., Ingvaldsen, R. B., Sperfeld, E., van Dijken, G. L., Stige, L. C., Olsen, A., and Ottersen, G.: Productivity in the Barents Sea – Response to Recent Climate Variability, Plos One, 9, e95273, doi:10.1371/journal.pone.0095273, 2014.

Gong, G.-C., Wen, Y.-H., Wang, B.-W., and Liu, G.-J.: Seasonal variation of chlorophyll *a* concentration, primary production and environmental conditions in the subtropical East China Sea, Deep-Sea Res. Pt. II, 50, 1219–1236, 2003.

Han, A. Q., Dai, M. H., Gan, J. P., Kao, S.-J., Zhao, X. Z., Jan, S., Li, Q., Lin, H., Chen, C.-T. A., Wang, L., Hu, J. Y., Wang, L. F., and Gong, F.: Inter-shelf nutrient transport from the East China Sea as a major nutrient source supporting winter primary production on the northeast South China Sea shelf, Biogeosciences, 10, 8159–8170, doi:10.5194/bg-10-8159-2013, 2013.

He, X., Bai, Y., Pan, D., Chen, C.-T. A., Cheng, Q., Wang, D., and Gong, F.: Satellite views of the seasonal and interannual variability of phytoplankton blooms in the eastern China seas over the past 14 yr (1998–2011), Biogeosciences, 10, 4721–4739, doi:10.5194/bg-10-4721-2013, 2013.

Ho, D. T., Law, C. S., Smith, M. J., Schlosser, P., Harvey, M., and Hill, P.: Measurements of air-sea gas exchange at high wind speeds in the Southern Ocean: Implications for global parameterizations, Geophys. Res. Lett., 33, L16611, doi:10.1029/2006GL026817, 2006.

Jiang, L.-Q., Cai, W.-J., Wanninkhof, R., Wang, Y.-C., and Luger, H.: Air-sea CO$_2$ fluxes on the US South Atlantic Bight: Spa-

tial and seasonal variability, J. Geophys. Res., 113, C07019, doi:10.1029/2007JC004366, 2008.

Kim, D., Choi, S.-H., Shim, J.-H., Kim, K.-H., and Kim, C.-H.: Revisiting the seasonal variations of sea-air CO$_2$ fluxes in the northern East China Sea, Terr. Atmos. Ocean. Sci., 24, 409–419, 2013.

Lalli, C. M. and Parsons, T. R.: Biological Oceanography: An Introduction. Butterworth Heinemann, Burlington, 48–73, 1993.

Laruelle, G. G., Durr, H. H., Slomp, C. P., and Borges, A. V.: Evaluation of sinks and sources of CO$_2$ in the global coastal ocean using a spatially-explicit typology of estuaries and continental shelves. Geophys. Res. Lett., 37, L15607, doi:10.1029/2010GL043691, 2010.

Laruelle, G. G., Lauerwald, R., Pfeil, B., and Regnier, P.: Regionalized global budget of the CO$_2$ exchange at the air-water interface in continental shelf seas, Global Biogeochem. Cy., 28, 1199–1214, 2014.

Lee, H. J. and Chao, S. Y.: A climatological description of circulation in and around the East China Sea, Deep-Sea Res. Pt. II, 50, 1065–1084, 2003.

Liss, P. S. and Merlivat, L.: Air-sea gas exchange rates: introduction and synthesis, in: The Role of Air-Sea Exchange in Geochemical Cycling, edited by: Buat-Menard, P., Reidel, Hingham, MA, 113–129, 1986.

Liu, Z. and Gan, J.: Variability of the Kuroshio in the East China Sea derived from satellite altimetry data, Deep-Sea Res. Pt. I, 59, 25–36, 2012.

Martinez, E., Antoine, D., D'Ortenzio, F., and de Boyer Montegut, C.: Phytoplankton spring and fall blooms in the North Atlantic in the 1980s and 2000s, J. Geophys. Res., 116, C11029, doi:10.1029/2010JC006836, 2011.

Martins, A. M. and Pelegri, J. L.: CZCS chlorophyll patterns in the South Atlantic Bight during low vertical stratification conditions, Cont. Shelf Res., 26, 429–457, 2006.

Omar, A., Johannessen, T., Kaltin, S., and Olsen, A.: Anthropogenic increase of oceanic pCO$_2$ in the Barents Sea surface water, J. Geophys. Res., 108, 3388, doi:10.1029/2002JC001628, 2003.

Peng, T. H., Hung, J. J., Wanninkhof, R., and Millero, F. J.: Carbon budget in the East China Sea in spring, Tellus B, 51, 531–540, 1999.

Pierrot, D., Neill, C., Sullivan, K., Castle, R., Wanninkhof, R., Luger, H., Johannessen, T., Olsen, A., Feely, R. A., and Cosca, C. E.: Recommendations for autonomous underway pCO$_2$ measuring systems and data-reduction routines, Deep-Sea Res. Pt. II, 56, 512–522, 2009.

Shim, J., Kim, D., Kang, Y. C., Lee, J. H., Jang, S. T., and Kim, C. H.: Seasonal variations in pCO$_2$ and its controlling factors in surface seawater of the northern East China Sea. Cont. Shelf Res., 27, 2623–2636, 2007.

Su, J.: Circulation dynamics of the China Seas north of 18 N coastal segment, in: The Sea (Vol. 11), edited by: Robinson, A. R. and Brink, K. H., John Wiley & Sons, Inc., New York, 483–505, 1998.

Sweeney, C., Gloor, E., Jacobson, A. R., Key, R. M., McKinley, G., Sarmiento, J. L., and Wanninkhof, R.: Constraining global air-sea gas exchange for CO$_2$ with recent bomb ^{14}C measurements, Global Biogeochem. Cy., 21, GB2015, doi:10.1029/2006GB002784, 2007.

Takahashi, T., Olafsson, J., Goddard, J. G., Chipman, D. W., and Sutherland, S. C.: Seasonal variation of CO$_2$ and nutrients in the high latitude surface oceans-A comparative study, Global Biogeochem. Cy., 7, 843–878, 1993.

Takahashi, T., Sutherland, S.C., Sweeney, C., Poisson, A., Metzl, N., Tilbrook, B., Bates, N., Wanninkhof, R., Feely, R. A., Sabine, C., Olafsson, J., and Nojiri, Y. Global sea-air CO$_2$ flux based on climatological surface ocean pCO$_2$, and seasonal biological and temperature effects, Deep-Sea Res. Pt. II, 49, 1601–1622, 2002.

Takahashi, T., Sutherland, S. C., Wanninkhof, R., Sweeney, C., Feely, R. A., Chipman, D. W., Hales, B., Friederich, G., Chavez, F., Sabine, C., Watson, A., Bakker, D. C. E., Schuster, U., Metzl, N., Yoshikawa-Inoue, H., Ishii, M., Midorikawa, T., Nojiri, Y., Kortzinger, A., Steinhoff, T., Hoppema, M., Olafsson, J., Arnarson, T. S., Tilbrook, B., Johannessen, T., Olsen, A., Bellerby, R., Wong, C. S., Delille, B., Bates, N. R., and de Baar, H. J. W.: Climatological mean and decadal change in surface ocean pCO$_2$, and net sea-air CO$_2$ flux over the global oceans, Deep-Sea Res. Pt. II, 56, 554–577, 2009.

Tans, P. P., Fung, I. Y., and Takahashi, T.: Observational constraints on the global atmospheric CO$_2$ budget, Science, 247, 1431–1438, 1990.

Tseng, C.-M., Liu, K.-K., Gong, G.-C., Shen, P.-Y., and Cai, W.-J.: CO$_2$ uptake in the East China Sea relying on Changjiang runoff is prone to change, Geophys. Res. Lett., 38, L24609, doi:10.1029/2011GL049774, 2011.

Tseng, C.-M., Shen, P.-Y., and Liu, K.-K.: Synthesis of observed air-sea CO$_2$ exchange fluxes in the river-dominated East China Sea and improved estimates of annual and seasonal net mean fluxes, Biogeosciences, 11, 3855–3870, doi:10.5194/bg-11-3855-2014, 2014.

Tsunogai, S., Watanabe, S., and Sato, T.: Is there a "continental shelf pump" for the absorption of atmospheric CO$_2$?, Tellus B, 51, 701–712, 1999.

Wang, B.-D., Wei, Q.-S., Chen, J.-F., and Xie, L.-P.: Annual cycle of hypoxia off the Changjiang (Yangtze River) Estuary, Mar. Environ. Res., 77, 1–5, 2012.

Wang, G., Dai, M., Shen, S. S. P., Bai, Y., and Xu, Y.: Quantifying uncertainty sources in the gridded data of sea surface CO$_2$ patial pressure, J. Geophys. Res. Oceans, 119, 5181–5189, 2014.

Wang, S.-L., Chen, C.-T. A., Hong, G.-H., and Chung, C.-S.: Carbon dioxide and related parameters in the East China Sea, Cont. Shelf Res., 20, 525–544, 2000.

Wanninkhof, R.: Relationship between wind speed and gas exchange over the ocean, J. Geophys. Res., 97, 7373–7382, 1992.

Wanninkhof, R., Doney, S. C., Takahashi, T., and McGillis, W.: The effect of using time-averaged winds on regional air-sea CO$_2$ fluxes, in: Gas Transfer at Water Surfaces, edited by: Donelan, M., Geophys. Monogr. Ser., Amrican Geophysical Union, Washington, D.C., 127, doi:10.1029/GM127p0351, 351–357, 2002.

Wanninkhof, R., Asher, W. E., Ho, D. T., Sweeney, C., and McGillis, W. R.: Advances in quantifying air-sea gas exchange and environmental forcing, Annu. Rev. Mar. Sci., 1, 213–244, 2009.

Weiss, R. F.: Carbon dioxide in water and seawater: the solubility of a non-ideal gas, Mar. Chem., 2, 203–215, 1974.

Weiss, R. F. and Price, B. A.: Nitrous oxide solubility in water and seawater, Mar. Chem., 8, 347–359, 1980.

Zhai, W.-D., Chen, J.-F., Jin, H.-Y., Li, H.-L., Liu, J.-W., He, X.-Q., and Bai, Y.: Spring carbonate chemistry dynamics of surface waters in the northern East China Sea: Water mixing, biological uptake of CO$_2$, and chemical buffering capacity, J. Geophys. Res. Oceans, 119, 5638–5653, doi:10.1002/2014JC009856, 2014.

Zhai, W.-D., Dai, M.-H., Chen, B.-S., Guo, X.-H., Li, Q., Shang, S.-L., Zhang, C.-Y., Cai, W.-J., and Wang, D.-X.: Seasonal variations of sea-air CO$_2$ fluxes in the largest tropical marginal sea (South China Sea) based on multiple-year underway measurements, Biogeosciences, 10, 7775–7791, doi:10.5194/bg-10-7775-2013, 2013.

Zhai, W.-D. and Dai, M.-H.: On the seasonal variation of air-sea CO$_2$ fluxes in the outer Changjiang (Yangtze River) Estuary, East China Sea. Mar. Chem., 117, 2–10, 2009.

Zhai, W.-D., Dai, M.-H., and Guo, X.-H.: Carbonate system and CO$_2$ degassing fluxes in the inner estuary of Changjiang (Yangtze) River, China, Mar. Chem., 107, 342–356, 2007.